A stand-alone micro heat pump for personalized environmental control system (PECS)

Building and Environment 284 (2025) 113476

Contents lists available at ScienceDirect

Building and Environment

journal homepage: www.elsevier.com/locate/buildenv

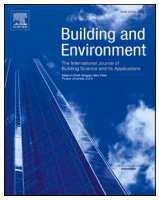

A stand-alone micro heat pump for personalized environmental control system (PECS)

V. Gentile *, M. Perino

TEBE Research Group, Department of Energy "G. Ferraris" (DENERG), Politecnico di Torino, Corso Duca degli Abruzzi 24, 10129, Torino, Italy

ARTICLE INFO

Keywords:
Thermal comfort
Personalized environmental comfort systems
PECS cooling
Micro heat pump
HC-290

ABSTRACT

This experimental study presents the design, development, and testing of a micro-scale vapor compression (VC) heat pump prototype tailored for novel Personalized Environmental Comfort Systems (PECS). The system employs a natural refrigerant (HC-290) to align with new environmental regulations, and integrates both compressor speed and expansion valve modulation, enabling continuous and precise control of cooling power and temperature – features rarely found in miniaturized systems. A key innovation is the integration of a 20-liter heat thermal energy storage unit (either sensible or latent) to buffer condensation heat and support standalone operation up to 8 h, without outdoor ducting or heat rejection. Experimental results show that localized cooling at approximately 20 °C can be maintained even in ambient conditions up to 36 °C, with an average Energy Efficiency Ratio (EER) of around 2 when using a latent heat thermal storage system based on phase change materials. The optimized configuration delivers a stable cooling output of ~200 W, sufficient to meet the thermal needs of a single occupant while minimizing the impact on indoor air conditions. By reducing the volume of conditioned space and enabling direct user-level control, the proposed system supports a shift toward decentralized comfort solutions, with the potential to relax central HVAC setpoints and reduce overall building energy consumption. The study also provides a comprehensive experimental characterization.

Symbols

EER	Energy Efficiency Ratio	
PECS	Personalized Environmental Comfort Systems	
TCC	Temperature Correction Capacity	
Φ	Heat flow rate	W
P_{el}	Absorbed electrical power	W
T	Temperature	°C
p	Refrigerant pressure	bar
β	Outlet/inlet pressure ratio at compressor	-
η	Efficiency	-
h	Enthalpy	kJ/kg
s	Entropy	kJ/kgK
Q_1	Water volume flow rate at evaporator	m^3/s
Q_2	Water volume flow rate at the condenser	m^3/s
$\dot{m}$	Mass flow rate	Kg/s
I	Compressor absorbed current	A
V	DC Compressor voltage supply	V_{DC}
c_p	Water specific heat capacity	kJ/kgK
Superscript/Subscript		
eva	at the evaporator	
cond	at the condenser	
H_2O	water	
HC-290	propane refrigerant	

(*continued on next column*)

(*continued*)

1. Introduction

Since the early 20th century, centralized air conditioning systems has been the dominant solution for ensuring thermal comfort during hot seasons. However, this approach presents intrinsic limitations: it provides uniform thermal conditions across entire rooms, failing to address individual comfort needs, and it requires significant energy by conditioning the full room volume, even though only a small portion is typically occupied. To overcome these inefficiencies, Personalized Environmental Comfort Systems (PECS) have been proposed as a more targeted and energy efficient alternative.

PECS are apparatuses that "can provide individually controlled thermal, air quality, acoustic or luminous environments in the immediate surroundings of an occupant, without affecting directly the entire

* Corresponding author.
E-mail address: vincenzo.gentile@polito.it (V. Gentile).

https://doi.org/10.1016/j.buildenv.2025.113476
Received 15 April 2025; Received in revised form 21 July 2025; Accepted 23 July 2025
Available online 29 July 2025

space and other occupants' environment " [1]. By enabling personal control over comfort parameters, such as temperature, air quality, lighting, and acoustic, PECS allow users to tailor their microclimate to individual preferences [2–5]. This flexibility can, in theory, reduce thermal discomfort to zero, surpassing the 5 % dissatisfaction threshold typical of centralized HVAC systems [6] and may also improve occupant productivity [7–11].

PECS also offer substantial energy-saving potential, a critical advantage in the context of climate change [12]. By conditioning only the space immediately surrounding the occupant, rather than the entire room volume, energy use can be significantly reduced while maintaining comfort. This is particularly effective in workplaces with intermittent and/or non-continuous occupancy. Several studies report notable energy savings achievable with PECS [13]. Verhaart et al. [14] estimated energy savings up to 34 % during the hot season, while other works show reductions from 4 % to 60 % when PECS allow ambient temperatures to deviate 4-5 K from standard set-points [15]. In cooling scenarios, typical savings range from 15 % to 20 %, with peaks of 50-60 % in specific cases [16–22].

In both heating and cooling modes, energy savings are achieved by relaxing background temperature control, by raising or lowering ambient setpoints, while preserving comfort through PECS [23]. To compensate, an additional heat flux, ΔL* (ideal supplementary power [24]), must be supplied locally.

ΔL* varies with air velocity (typically ranging from 0.1 to 0.9 m/s) and the background operative temperature(T_{op}): during the heating season, it ranges from 0 to 140 W as T_{op} drops from 23 °C to 8 °C; during the cooling season, it ranges from 0 to -100 W, as the T_{op} rises from 23 °C to 34 °C. Even with low-efficiency[1] devices, the required power remains below 500 W, far less than that of typical centralized HVAC units.

PECS can be categorized according to the nature of conditioning action exerted on occupants [13]. Limiting the analysis only to those devices operating thermo fluid dynamic actions (hence excluding acoustic, lighting, and IAQ), five typologies can be identified.

1.1. PECS classification

1) *Heating PECS*: used in heating-dominated spaces with indoor air temperatures between 10 and 18 °C. These systems warm the whole human body or targeted areas via heat radiation and conduction, without air movement. Examples include heated chairs, carpets, footwarmers, local radiant panels, and hand warmer [25–30].
2) *Heating and Ventilation PECS*: also for heating-dominated environments, but suitable for broader temperature ranges (below or above 20 °C). They combine convection, radiation, and conduction, offering greater user control and more uniform heat distribution (often preferred for thermal comfort). Typical examples are the fan heaters.
3) *Cooling PECS*: designed for cooling-dominated buildings (typically 28-32 °C, up to 34 °C), these systems remove heat from the human body via radiation and conduction, without airflow. Examples include cooled chairs, carpets and local radiant panels.
4) *Ventilation PECS*: most common in cooling-dominated buildings, typically used at 23-28 °C (rarely above 30 °C). These devices do not cool the air, but increase air velocity to enhance heat loss and evaporation, producing cooling a sensation. For this reason, also known as "*isothermal cooling*" devices. Typical examples include ceiling fans, stand/table/box fans, desk fans, ventilated chairs, and isothermal jets (e.g., nozzle, slot diffuser in desk or partition) [31–35].
5) *Cooling and Ventilation PECS*: operate in similar temperature ranges as cooling PECS, but supply slightly cooler fresh air than the ambient via convective jets, improving cooling efficiency. Often use nozzles or diffusers like those in ventilation PECS.

1.2. Temperature correction capacity and PECS efficiency

1.2.1. Heating, heating and ventilation

To evaluate PECS performance, Zhang et al. [23] introduced the concept of "*Corrective Power*" (CP), later refined by Perino et al. [24] as the "*Temperature Correction Capacity*" (TCC) . The TCC quantifies the temperature difference required to achieve the same comfort level with and without PECS, assuming all other conditions remain unchanged. In heating mode (where data availability is lower), TCC values range from +7 K to +10 K for heated chairs and from +2 K to +6 K for foot, leg, or hand warmers [23], often powered by Joule-heated metallic or ceramic elements [36–38].

"*Heating and ventilation PECS*", such as fan heaters, are widespread but less efficient. Convective heating increases air velocity, which can intensify heat losses from the body, requiring higher air jet temperatures to maintain comfort. Despite achieving TCC values similar to "*Heating PECS*" (e.g., TCC from +7 K to +8 K [24]), their *Temperature Correction Capacity Efficiency* (TCCE) is low, around 150 W/K. Where the TCCE is the heating/cooling power needed to produce ±1 K of temperature correction[2].

Whether heating or heating and ventilation PECS are used, both categories require thermal energy transfer via air or other fluids, commonly using electric resistance heating—a simple, low-cost but inefficient method from a thermodynamic standpoint. In addition to their low energy efficiency, these systems do not offer any control over humidity, often producing overly dry airflows that may further compromise thermal comfort, particularly during prolonged use or in already dry environments.

1.2.2. Cooling, ventilation, cooling and ventilation

Cooling mode has been more extensively explored, yielding a broader dataset on performance [13],[23],[39]. Among the various approaches, "*Ventilation PECS*" are the most widely adopted due to simplicity and ease of installation. However, as Zhang et al. [23] noted, the TCC of isothermal convective cooling is modest and highly dependent on local air velocity near the skin. Key findings include:

- at background temperature (T_{back}) of 26-27 °C, and local air speeds of 0.36-0.60 m/s, TCC ranges from -1 K to -3 K;
- at T_{back} of 28 °C, and local air speeds of 0.40-0.60 m/s, TCC ranges from -2 K to -3 K;
- at T_{back} of 30 °C, and local air speeds of 0.80-1.00 m/s, TCC ranges from -2 K to -4 K;
- at T_{back} of 32 °C, at least 2.00 m/s are required for comfort, yielding a TCC of -4 K to -5 K;
- above T_{back} of 32 °C, isothermal air cooling alone is insufficient to assure comfort.

Ceiling and box fans offer similar performance, often achieving 1-2 K greater TCC than frontal air jets at equal conditions. Ceiling fans, for instance, can ensure comfort up to a T_{back} of 33 °C. Rawal et al. reported similar findings[13], where most "*Ventilation PECS*" achieve TCC values between -2 K and -4 K, with few cases reaching -6 K at the cost of significantly higher local air velocities. Users, typically tend to increase local air velocity when in control, often up to 0.90 m/s [16],[40],[41], with rare cases reaching 3.00 m/s [42]. However, excessive air velocities may cause localized discomfort [43],[44]. In summary, frontal air jets and fans typically provide -3 K TCC when local air speeds range from 0.30 to 0.60 m/s, which can be increased to –5 K if airspeed reaches up

[1] The PECS energy efficiency is defined as[24]: $\eta_{PECS} = \frac{\Delta L^*}{\Phi_{PECS}}$, where Φ_{PECS} is the actual heating/cooling power that is absorbed by the PECS.

[2] The smaller the TCCE value, the higher the energy efficiency of the device is.

to 0.60-1.00 m/s.

Achieving greater TCC requires additional air jet cooling, making "*Cooling and Ventilation PECS*" necessary. For instance, lowering supply air temperature by 2-5 K can further enhance TCC by -2 to -3 K. Cooled air jets typically supply air at 19-25 °C [45], with temperature differences of up to -2.5 °C between the background and micro-environment [42],[46]. Nonetheless, although isothermal convective cooling can achieve appreciable TCC values, its effectiveness is ultimately limited by two critical factors. First, air velocities above 1.5 m/s—often required to enhance performance—can lead to localized discomfort and are generally not acceptable for prolonged exposure. Second, and perhaps more importantly, isothermal cooling offers no means of controlling humidity. In humid environments, this lack of dehumidification can drastically reduce its cooling effectiveness, making it unsuitable for maintaining comfort under such conditions.

The highest TCC values in cooling mode are achieved with "*Cooling PECS*." For example, cooled chairs easily provide a TCC of -5 K, while air sleeves, cooled seats, radiant panels, and phase-change garments can maintain comfort even when T_{back} reaches 30-32 °C.

1.2.3. Personal thermal management systems (PTMS)

To enhance mobility and bring thermal control closer to the body, *Personal Thermal Management Systems* (PTMS) have been proposed [39]. These systems are, in theory, more energy-efficient than conventional PECS [24], with active devices typically consuming <30 W [39]. PTMS include both passive and active solutions: passive systems regulate heat exchange by altering fabric and garments properties, while active systems integrate heating/cooling elements that directly influence body heat balance. Heating is commonly achieved using electric resistive elements (e.g., wires, fabrics) or thermoelectric devices, which can also enable cooling. Cooling techniques include evaporative cooling (EC), phase change materials (PCM), thermoelectric cooling (TEC), liquid cooling (LC), and air cooling (AC) [39]. While EC is extensively used outdoors and could theoretically enhance "*Ventilation and Cooling PECS*", it is unsuitable for indoor applications due to increased latent loads and humidity. In contrast, AC and LC-based PECS require pre-cooled air or a cold heat carrier fluid.

1.2.4. Challenges in heating and cooling PECS

The state of the art analysis shows that many types of PECS require air or other fluid to be cooled or heated. However, directly applying traditional solutions like chillers/heat pumps is impractical. Standard HVAC technologies rely on extensive ducting and wiring, which limits occupant mobility, reduces flexibility, and complicates building maintenance operations. Additionally, few commercially available cooling/heating systems provide thermal output in the range needed for PECS (e.g., 100 - 200 W).

Thermoelectric cooling (Peltier-based) has been explored as a compact, static, ductless solution. However, its cooling capacity is often inadequate, and disappointing results are frequent. For example, a 48 W Peltier element integrated into an air terminal device (a local air jet) achieved negligible TCC of -0.3 K, dissipating rejected heat via water pipes [47–49]. Similarly, Zhao et al. [50] developed a portable thermoelectric energy conversion unit (TECU) for PTMS with a cooling power limited to 2-15 W (again treating a small air flow). However, its EER was quite poor (0.58 at 10 W of cooling) and the maximum TCC was limited to –2 K.

Considering this background, standalone appliances with a cooling/heating capacity of 100-500 W, minimal environmental impact, and good energy efficiency are necessary. These key points represent the main challenge for future research in the PECS field. In addition, due to their low efficiency and limited cooling capacity, Peltier-based technologies for the same reason of low efficacy and cooling capacity, would result inadequate in the eventual control of the RH surrounding the human body.

A promising development path involves compact inverse Vapor Compression (VC) systems. These small-scale multifunctional heat pumps use miniaturized compressors with electric power absorption comparable to isothermal fan coolers. They can operate with natural and environmentally friendly refrigerants, like propane (HC-290).

Nonetheless, VC-based PECS face a major challenge: heat rejection.

Outdoor heat discharge requires cumbersome ducting and compromises the stand-alone requirement. On the other hand, indoor dissipation could lead to discomfort (overheating/overcooling) or energy inefficiency as centralized HVAC systems (if present) must compensate for this heat rejection (even if it's a small power compared to typical building cooling/heating loads).

An alternative approach involves storing the rejected heat on board when the equipment is operating during the occupancy time and releasing the stored heat indoors/outdoors during off-peak hours (e.g., 8 PM to 8 AM). This strategy appears optimal if applied to PECS, whose use is inherently designed to be intermittent and "on demand" (only when and where people occupy their position/workplace). The heat storage must be designed to accommodate the heat rejected during about 6-8 hours of operation, without being overly bulky. An innovative solution to manage heat rejection in compact vapor compression systems, especially when outdoor dissipation is not viable, involves integrating small-scale thermal energy storage (TES or LHTES) units. This approach allows temporary heat buffering, enabling ductless operation and supporting portable or desk-integrated deployment. While a few studies have investigated the use of PCM in the LHTES configuration for PECS applications [51–58] the coupling of micro heat pumps with PCM-based LHTES for personal comfort applications is underexplored. In addition, despite these studies confirm the potential of PCM-based solutions systems, they highlighted open issues related to long-term cycling performance, integration complexity, and control strategies. Ling et al [2] proposed a ductless, portable PECS called Roving Comforter (RoCo), featuring a 150 W micro-HP that rejects waste heat into a PCM storage. RoCO can provide 8 hours of conditioned air, lowering the supply air temperature by 4 K (e.g., 19 °C supply vs 23 °C in the background environment). While RoCo represents an interesting example of innovative "Ventilation and Cooling" or "Cooling PECS", a systematic research activity on this kind of appliance is still lacking. Several questions about feasibility and performance are still open. Moreover, RoCo relied on an R134a-heat pump system, which conflicts with current EU "F-gases" regulations [59].

1.3. Research objectives

A compact water-to-water VC unit, operating with a natural and environmentally sustainable refrigerant (HC-290), was conceived, designed, and built to address the critical limitations of current PECS technologies. The prototype was developed specifically for integration into a stand-alone PECS, with particular attention to regulatory compliance and environmental impact. A key feature of the system is its dual active control strategy, which enables continuous and independent modulation of compressor speed and expansion valve aperture. This architecture allows for real-time tuning of both cooling power and supply temperature, offering a high degree of flexibility and adaptability to user needs, an innovation not found in comparable PECS systems.

The micro-heat pump can be coupled with either a TES or a LHTES unit based on PCM, enabling onboard heat rejection and supporting autonomous operation for several hours.

This paper presents the design rationale, technical implementation, and an extensive experimental characterization of the prototype. The results, spanning from steady-state to dynamic operating conditions, provide unprecedented insight into the energy efficiency, performance range, and controllability of VC-based PECS systems.

2. The micro-HP design and development

2.1. Generalities

Fig. 1 schematizes the working principles of an active PECS integrated with a centralized HVAC system. Here, "active" indicates that the unit actively heat or cools a heat carrier fluid to a temperature different from the background ambient (T_a). This category includes PECS units for heating, cooling, and ventilation. An active PECS typically comprises:

i) a thermal interface that transfers the supplementary power (ΔL^*) to the human body through convection, radiation, or conduction [24];
ii) a thermal unit that generates fluid (usually air) at a suitable temperature (T_j), relative humidity (RH_j), and velocity (v_j).

While much of the literature has focused on improving the interface with the occupant, little attention has been paid to developing compact heating/cooling units suited to PECS applications. To fill this gap, our research explores viable thermal generation technologies.

Table 1 compares five heating/cooling strategies, summarizing their pros and cons. Evaporative and desiccant cooling present humidity-related challenges or limited thermal control. Thermoelectric solutions, such as Joule and Peltier devices, offer miniaturization potential but suffer from low efficiency and limited capacity. Among the options, VC heat pumps stand out due to their higher energy efficiency and flexibility in output temperature regulation. Moreover, the temperature levels at which the heat carrier fluid is produced can be varied within a relatively wide range with minor adjustments of the operative parameters of the cycle. This feature is very important since:

- it makes the system versatile and suitable to be coupled with various heat transfer interfaces (e.g., heated/cooled chairs, carpets, panels, air jets, heating/cooling fans),
- it allows an ample range of regulation and, consequently, occupants can widely personalize their comfort conditions, such as T_j, and, eventually, RH_j, v_j.

Therefore, in principle, VC heat pumps seem to stand out as the most promising, flexible, and energy-efficient solution for active PECS. The major drawbacks of this technology are the need to reject a certain amount of heat to the environment, and the difficulty of finding commercialy available apparatuses suitably sized for the power levels required by a PECS.

To address these limitations, a compact and stand-alone micro heat pump (micro-HP) prototype was developed. The system was designed to:

- operate without ducting or hydronic connections;
- allow user-level control of temperature and thermal power;
- function without direct heat rejection to the outdoor environment;
- minimize the adverse effects of indoor heat rejection.

This study focuses on the cooling performance of the micro-HP, though the system is fully reversible and capable of heating operation as well.

2.2. Prototype structure and features

The proposed prototypal micro-HP is based on a single-stage inverse vapor compressor cycle and is equipped with an adjustable lamination valve that acts on the refrigerant pressure at the evaporator (picture of the prototype in Fig. 2a). This feature allows for controlling the minimum temperature of the cooling cycle. Likewise, a compressor with adjustable rpm is adopted to regulate the refrigerant flow in the circuits and to vary the total exchanged heat at the evaporator (i.e., the cooling power). In particular, the expansion valve is electronically controlled and can adjust the aperture of the orifice by varying the diameter between 0 and 0.8 mm in 500 regulation steps. The compressor is a twin rotary compressor driven by a 48 VDC motor, having the possibility of modifying the rotation speed, linearly, from 1800 to 6000 rpm (which corresponds to an absorbed electrical power from 20 to 200 W). The RPMs are modulated by changing the resistance (between 1 and 50 kΩ) of a potentiometer connected to the compressor controlling shield.

Particular care was paid to the choice of the refrigerant fluid. Starting from 2025 [59], the European Regulation 2024/573 forces a mandatory phase-down of hydrofluorocarbons (HFCs) with a Global Warming Potential (GWP) greater than 150. This regulation aligns with the global shift towards reducing the environmental impact of refrigeration gases. While hydrofluoroolefins (HFOs), with ultra-low GWP, were initially considered as potential replacements of HFCs, their short atmospheric lifespan leads to the rapid formation of persistent organic pollutants, which makes them subject to restrictions under the upcoming PFAS (PerFluorinated Alkylated Substances) regulations. These concurrent limitations on HFCs and HFOs will likely drive the refrigeration industry toward adopting flammable refrigerants.

In agreement with these trends, it was decided to use the HC-290 (propane gas) as a refrigerant in the micro-HP prototype. HC-290, classified under the A3 flammability risk class, has a GWP of 0.02,

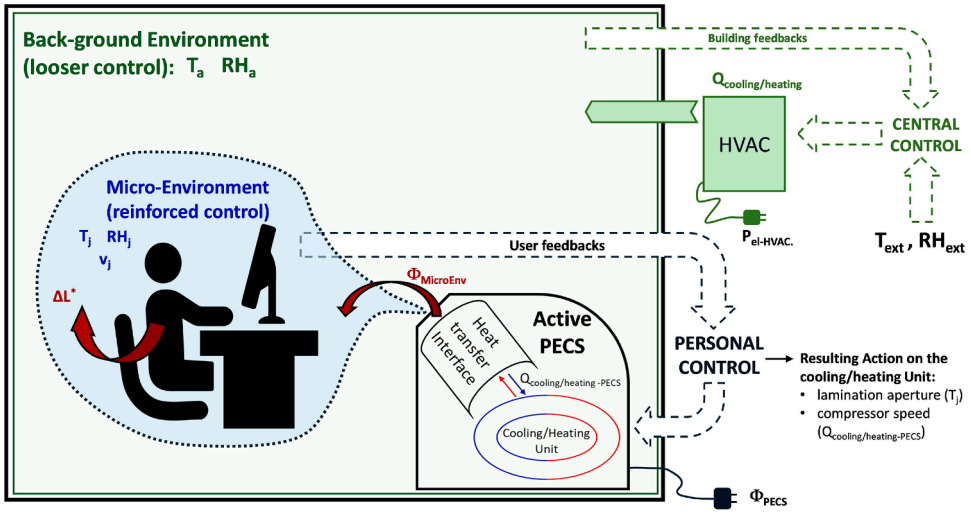

Fig. 1. Working principles and sub-systems of PECS.

Table 1
Possible cooling/heating technology for active PECS.

Technology Category	Control action on:			Φ/P_{el}		Cons	Pros
	T_j	RH_j	v_j	heating	cooling		
isothermal convection	none	none	relevant	-	>1	- limited TCC in cooling - higher TCC at very high air speed	- low energy consumption - flexible integration
Joule effect	relevant	none or pejorative	only with fans	0.1 - 0.5	-	- limited to heating - energy intensive	- wearable integration - potentially no limits on TCC in heating
Peltier effect	limited capacity in cooling	limited	only with fans	<1	0.1 - 0.5	- requires a support media surface for heat transfer - requires heat rejection - low-density power - limited air temperature reduction/ increase	- high level of miniaturization for localized cooling on small body areas - no ducting - static unit (mainly, fans are usually needed to enhance the heat transfer) - can be used in heat transfer interfaces, exploiting whichever heat transfer mechanism*
evaporative cooling	wet bulb limitation	pejorative	only with fans		>1	- increase the relative humidity of the surrounding environment - requires water-feeding - may degrade IAQ - can only be used in heat transfer interfaces based on convection	- high efficiency - highly portable
desiccant	none	relevant	only with fans		<1	- requires electricity for material regeneration - low energy efficiency - no control over the temperature - can only be used in heat transfer interfaces based on convection	- highly effective on skin evapotranspiration - high level of miniaturization - possible implementation in clothing
heat pump	both cooling and heating	relevant	only with fans	>1	>1	- requires heat rejection - requires ducting - requires miniaturization for portable devices	- highly effective in local temperature and humidity control - high energy efficiency - low power consumption - large air temperature reduction/increase - easy to adjust the temperature levels - can be used in heat transfer interfaces, exploiting whichever heat transfer mechanism*

* Conduction, convection, radiation.

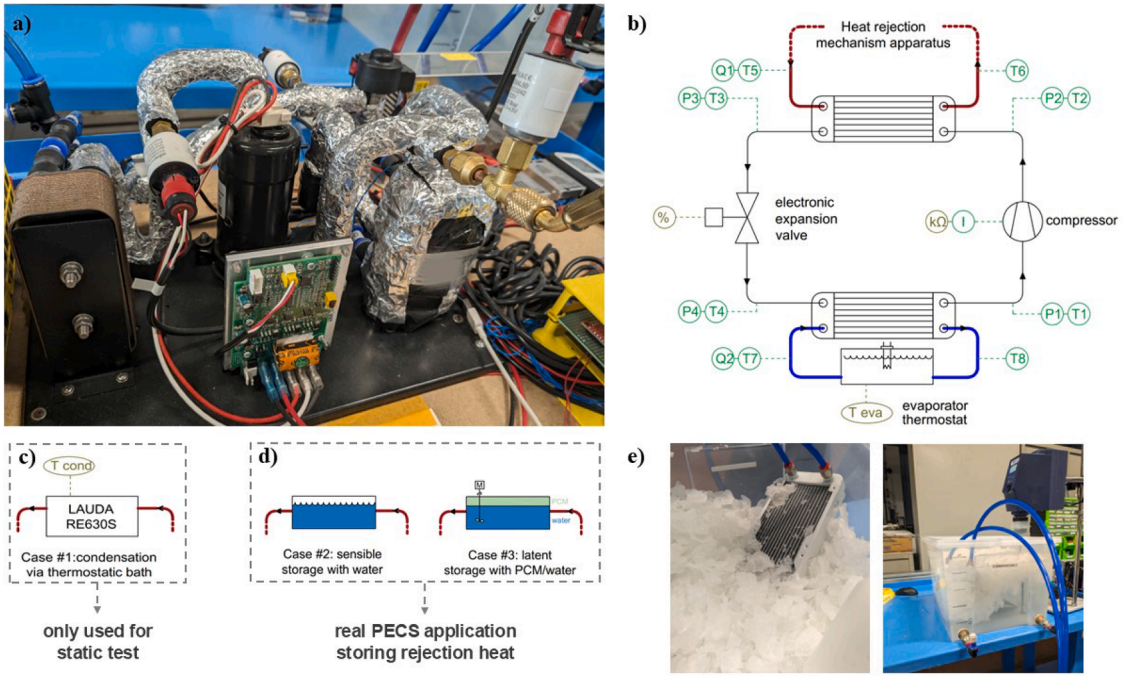

Fig. 2. (a) Photograph of the heat pump prototype. (b) Experimental setup showing different heat rejection configurations. In (c), condensation is done using water and a LAUDA RE630S thermostatic bath, while in (d) condensation heat is stored through sensible (water) or latent heat (PCM) exchange, respectively. (e) Photograph of the PCM, the heat exchanger, and the mixer used to obtain the configuration of the Case #3.

making it an environmentally favorable option. It has an autoignition temperature of 470 °C and a lower flammability limit (LFL) of 0.038 kg/m^3 (equivalent to 2.1 % v/v in dry air) [60].

Recent updates to the safety standards for refrigerating appliances in residential buildings set strict guidelines on the maximum allowable charge of flammable refrigerants. These standards limit the total amount of HC-290 to up to 13 times its LFL based on the system's circuit internal volume, with a maximum allowable charge of 1.2 kg. Moreover, more stringent safety requirements, such as the selection of welding materials, temperature tolerances, and pressure limits, apply if the system contains more than 150 grams of flammable refrigerant [61].

Such constraints constitute a challenging barrier to develope air conditioning units designed to be applied to rooms, flats, and/or entire buildings because the power in play requires refrigerant charges that often exceed these limits.

On the other hand, the field of PECS appears to be a natural candidate for the successful application of vapor cycles using flammable refrigerants.

In the case of the proposed prototype, the amount of HC-290 necessary to provide a cooling capacity of several hundred watts is relatively small and comparable to the mass of propane that is contained in few standard portable gas lighters (approximately 10 grams per lighter [62]). This makes the HC-290 a viable and optimal choice.

By varying the charge of the refrigerant and the pressure levels at the evaporator and condenser, the temperatures at which "heat" and "cold" are exchanged can be varied to some extent.

Since the future idea is to integrate the micro-HP in a *cooling and ventilation* and/or *cooling* PECS, the lower temperature of the heat carrier fluid was chosen to be around 20 °C (or somewhat below).

Finally, two heat exchange apparatuses, one for the evaporator and one for the condenser, were designed.

At this research stage, the attention was focused on exploiting only the cooling side of the heat pump. For these reasons, the evaporator has been designed adopting a very traditional structure (typical of the water-to-water heat pump), that is a miniaturized plate heat exchanger. The cooling load is simulated using a thermostated water flow on the secondary side of the heat exchanger. Instead, various configurations were designed and tested for the condenser. This is because the heat exchanged in this component represents, in a real application, the thermal energy that must be rejected towards the environment.

The first configuration (case #1 in Fig. 2c) mirrors the evaporator structure based on a plate heat exchanger. This, again, would be the typical solution for a water-to-water heat pump working in a quasi steady-state regime. The rejected heat is then removed using a thermostated water flow. In such conditions, the temperature at which the condensation occurs is fixed, can be controlled, and is constant over time. This configuration was used to test the efficiency of the VC cycle in reference conditions (to compare its performance with those of chillers available on the market).

However, as previously highlighted, this solution, if applied to a PECS, has the great disadvantage of requiring the management of the rejected heat. Thus, it most likely needs extensive ducting. To avoid such a drawback, two different alternative configurations were conceived and tested. The base idea is to operate the heat pump in a non-steady state, buffering the rejected thermal energy at the condenser using miniaturized heat storages. For case #2, the choice fell on a sensible heat Thermal Energy Storage (TES) consisting of a 20 liter water reservoir (Fig. 2d). Alternatively, case #3 uses a Latent Heat Thermal Energy Storage (LHTES) of equivalent volume, which combines water and a suitable PCM (Fig. 2d). In particular, Rubitherm RT35HC PCM was used, with a melting temperature between 34 and 36 °C and a heat storage capacity of 240 kJ/kg within the 27-42 °C temperature range [63]. Despite the fact that a lower phase transition temperature would improve the overall energy efficiency of the heat pump and the system, a melting temperature around 35 °C was selected to ensure reliable re-solidification of the PCM via passive heat exchange with the surrounding environment, thus guaranteeing full storage availability even under unconditioned background conditions. In this preliminary prototype, to enhance heat transfer between the water, the PCM, and the microchannel heat exchanger connected to the micro-HP, a mechanical stirrer rotating at 200 rpm was used to continuously mix the water and prevent the formation of boundary layers. Features of sensors and components are shown in paragraph 3.2. The 20 liter capacity was selected as an upper limit to allow seamless integration of the TES/LHTES unit into a standard desk layout, maintaining both the visual appeal and functional usability of the workspace.

With condensers of cases #2 and #3, the VC system does not operate continuously but follows a working cycle. During the active phase, the PECS cools while storing the rejected heat into the TES/LHTES. During the off phase, the stored heat is passively released, resetting the TES/LHTES to their initial state. The condensation temperature is not fixed or strictly controlled from the thermodynamic perspective. In the case of TES, the condensation temperature gradually increases, limiting the operability of the VC cycle to a certain duration. As the outlet temperature of the compressor rises, it eventually reaches a safety threshold, at which point the compressor must be halted.

Using the LHTES technology the operating time can be extended. In this case, the rejected heat is stored at a nearly constant temperature corresponding to the transition phase of the PCM. Only after the entire PCM mass has fully melted does the condensation temperature begin to rise, ultimately requiring the compressor to stop.

3. Performance evaluations

3.1. The test plan

An extensive experimental campaign was conducted to assess the micro-HP's performance across various configurations and operating conditions. The experiments were divided into two groups, each with distinct objectives.

The first set of tests ("static tests" using configuration #1, as shown in Fig. 2c) focused on evaluating the VC cycle under reference and steady-state conditions at the evaporator and condenser. These tests provided a baseline for comparing the nominal performance of the micro-HP with similar products, supporting labelling and ranking purposes. The experiments kept the cooling service at 20 °C, while adopting the condenser configuration #1. The measured quantities included the condensation temperature (which varied from 25 °C to 33 °C) and the aperture of the lamination valve. Table 2 summarizes the key parameters of these tests, with each test labelled sequentially.

The static tests were performed to analyze four distinct operating phases of the micro-HP:

- *Starting Phase*: during this initial stage (typically under 3 min), the HP remains inactive while the water circulators for the evaporator and condenser operate. This ensures temperature equilibration between water and refrigerant throughout the loop, stabilizing the system under the predefined test conditions.
- *Transient Phase*: the compressor is powered on, initiating a transient period during which its rotational speed stabilizes. During this phase, refrigerant temperatures and pressures vary significantly over time.
- *Stationary Phase*: once transient effects run out, and both pressure and temperature stabilize, steady-state performance evaluation begins. The duration of this phase is set to collect a sufficient number of data points for a statistically significant assessment of the Key Performance Indicators (KPIs, reported in paragraph 3.2).
- *Phase Down*: the compressor is switched off while the water circulators in the evaporator and condenser continue running. The system's thermal behavior is monitored to analyze the final re-equilibration of the hydronic circuit.

In the second stage of the research, the focus shifted towards

Table 2
Static Tests with the condenser configuration #1 and the thermostat LAUDA.

Thermostat evaporator	Thermostat condenser	Compressor speed	Expansion valve aperture						
[°C]	[°C]	[rpm]	90%	80%	70%	60%	50%	40%	30%
20	25	2120	#1	#2	#3	#4	#5	#6	#7
20	28	2120	#8	#9	#10	#11	#12	#13	#14
20	31	2120	#15	#16	#17	#18	#19	#20	#21
20	33	2120	#22	#28	#23	#24	#25	#26	#27

evaluating the micro-HP's performances in a stand-alone configuration designed for PECS, using condenser arrangements #2 and #3 (Fig. 2d). The objective was to assess the prototype's behavior under realistic office environment conditions. Unlike the static tests, these experiments involved inherently non-steady state operation. A key factor in these tests was to determine the maximum time period for which the appliance can operate, beyond standard KPIs, before the condensing temperature reaches levels that could compromise the compressor's safe operation. Measurements were repeated for both the TES and LHTES condenser configurations. Test conditions are summarized in Table 3 for case #2 (TES) and Table 4 for case #3 (LHTES).

3.2. The experimental test rig and the adopted KPI

The prototype of the stand-alone micro-HP was installed in a suitable test circuit, as shown in Fig. 2b, with sensors positioned to monitor key parameters. Refrigerant temperatures were measured at the four key points of the VC cycle (T_1 to T_4 with ±2 % accuracy between -55 °C and 155 °C). The temperature probes are attached to the copper pipes (6 mm inner diameter) using conductive solder paste and thermally insulated from the surrounding environment. This setup minimized thermal resistance and assured accurate temperature readings of the refrigerant. Four pressure transducers (P_1 to P_4 in Fig. 2b, with ±1 % accuracy within -40 °C and 120 °C) were directly threaded into the copper pipes at the same locations as the temperature sensors, allowing simultaneous pressure and temperature measurements at these key points. To assess heat transfer performance, the energy balance was solved at the plate heat exchangers' secondary circuit (water loop). Water flow rates in the secondary loops (Q_1 and Q_2) were measured using an electromagnetic flow meter with ±1.5 % accuracy, together with the temperature differences at the inlets and outlets ($\Delta T_{cond} = T_6–T_5$ and $\Delta T_{eva} = T_7\text{-}T_8$). The electrical power consumption of the compressor and auxiliary components was determined by measuring the current draw by the device with ±1.5 % of accuracy. Table 5 summarizes the experimental setups and sensors' main features.

The KPI and metrics assessed during the experimental campaign are summarized in Table 6. A critical parameter that must be carefully monitored is the compressor outlet temperature (T_2 in Fig. 2b), which indicates the compressor's safe operation and proper health. Excessively high outlet temperatures can lead to thermal degradation of the lubricant required for safe propane compression. Additionally, this temperature and the compression ratio are closely linked to energy consumption, as they directly influence the theoretical work of compression and, consequently, the system's overall electrical consumption.

Other important KPIs for evaluating the system operation include the isentropic efficiency of compression (η_{iso}) and the time required to reach a steady state condition (t_{steady}). The latter is particularly relevant for applications where the micro-HP operates under variable conditions. From an energy performance perspective, the heat flow rate exchanged at the evaporator is crucial for two reasons: first, to determine whether the system meets the personal cooling demand (ΔL^*), and second, to assess the amount of heat that must be rejected. Finally, the system's overall efficiency is evaluated by assessing the EER (Energy Efficiency Ratio) by integrating the ratio of the heat exchanged at the evaporator and the electrical absorption.

Table 3
Tests for PECS application - condenser configuration #2 (TES).

Test	HC-290 mass	Compressor speed	Condenser Volume	T evap.	T storage initial	T storage final
-	[g]	[rpm]	[l]	[°C]	[°C]	[°C]
#29	61.2	3060	5	22	22	36
#30	61.2	3480	5	22	22	
#31	61.2	4320	5	22	22	
#32	61.2	5580	5	22	22	
#33	61.2	2640	20	20	20	
#34	61.2	2640	20	27	27	
#35	61.2	2220	20	27	27	
#36	61.2	2220	20	20	20	
#37	38.9	3480	20	20	20	
#38	38.9	2220	20	20	20	
#39	38.9	2220	20	27	27	
#40	38.9	2220	20	20	20	
#41	38.9	2220	20	27	27	

4. Experimental results

4.1. Static tests - performance with a thermostated condenser (case #1)

Table 7 resumes the main results obtained during the 27 static tests, which were done for different boundary and operative conditions. Each test comprised the four distinct operational phases described in Section 3.1. The results shown in Table 7 are the mean values of the relevant parameters averaged over the *stationary phase*.

As it is possible to see, the cooling power varied between a maximum of about 250 W to a minimum of about 100 W, which aligns perfectly with the cooling demand of a PECS [24]. The corresponding EER ranged from a very high value of 5.8 for test #1 to an unfavorable minimum of 1.1 for test #27 (that corresponds, respectively, to an average condensing temperature of about 26.3 °C and a 10 % aperture of the lamination valve for #1 and 32.5 °C and 70 % for #27). The rejected heat flow rate, Φ_{cond}, spanned from about 220 W to 350 W. Since the compressor rotational speed was the same for all the tests, reducing the lamination valve aperture directly reduced the HC-290 refrigerant flow rate circulating in the micro-HP, thereby lowering heat exchanges at both the evaporator and the condenser.

Fig. 3a, b and c show the trend of the EER, cooling power (Φ_{eva}) and rejected heat flux (Φ_{cond}) versus the aperture percentage of the lamination valve (0 % corresponds to a fully close valve and 100 % to a fully open) for various water temperatures at the condenser (constant nominal values respectively equal to 25 °C, 28 °C, 31 °C, and 33 °C). In these tests, the evaporator inlet water temperature was kept constant at 20 °C using a thermostatic bath, simulating a cooling load on the PECS. Such temperature levels at the evaporator and condenser correspond to a theoretical TCC of the PECS equal to -5 K, -8 K, -11 K, and -13 K, respectively.

As expected, increasing the temperature difference between the evaporator and condenser lowers Carnot's efficiency, resulting in a drop in the actual EER.

The optimal regulation range for the lamination valve is observed between 60 % and 85 % of aperture, where the EER reaches its peak

Table 4
Tests for PECS application - condenser configuration #3 (LHTES).

Test -	HC-290 mass [g]	Compressor speed [rpm]	PCM mass [kg]	Water mass [kg]	Mixing speed [rpm]	T storage initial [°C]	T storage final [°C]
#42	38,9	2220	5	15	1400	25	36
#43, #44, #45	38,9	2220	5	15	1400	25	36

Table 5
Features of the micro-HP prototype and specs of sensors used to measure temperatures, pressure, mass flows, and current.

Sensor Label	Specs	Monitored Parameter
T1, T2, T3, T4	NTC thermistor; R25°C=10kΩ; err ±2%; -55°C - 155°C;	HC-290 temperature
P1, P2, P3, P4	Pressure transducer; 0-34.5 bar; err ±1%, -40°C - 120°C	HC-290 relative pressure
T5, T6, T7, T8	NTC thermistor; R25°C=10kΩ±2%; -55°C - 155°C;	Hot and cold water temperature
Q1, Q2	Electromagnetic flowmeter; 0.2-20L/min; err ±1.5%	Hot and cold-water flow rate
I	Hall-effect based linear current sensor ACS712; err ±1.5% at ±30A and 25°C	Absorbed Current by actuators
Compressor	twin rotary compressor with a 48VDC motor (20-200 W), variable speed 1800-6000 rpm	
Expansion	PTFE electronic expansion valve with 500 regulation steps and 0.8 mm orifice.	
Evaporator	Brazed plate heat exchanger with 12 plates (117 × 50 × 25 mm)	
Condenser	Brazed plate heat exchanger with 32 plates (117 × 54 × 41 mm)	

Table 6
KPI used for analysis of test results.

Parameter		Unit	Description	Equation
Focused on PECS application performances	EER	-	Energy efficiency ratio	$\int_{t_{in}}^{t_{fin}} \Phi_{eva(t)}/P_{el(t)} * dt$
	Φ_{eva}	W	Exchanged heat at the evaporator	$Q_1 * \rho_{H_2O} * c_p(T_7 - T_8)$
	Φ_{cond}	W	Exchanged heat at the condenser	$Q_2 * \rho_{H_2O} * c_p(T_6 - T_5)$
Focused on refrigeration cycle performances	P_{el}	W	Electric absorption	$I * V$
	T_2	°C	Outlet compressor temperature	-
	β	-	Refrigerant compression ratio between evaporator and condenser	p_2/p_1
	η_{iso}	-	Isentropic efficiency of compression	$(h_{2is} - h_1)/(h_2 - h_1)$
	t_{steady}	[minutes]	Time required for reaching the steady state regime of the heat pump	$t_{\left\lvert\frac{dT_2}{dt}\right\rvert<1\%}$

values (ranging from about 2 to 5, depending on the condenser's temperature). This range of operation for the lamination valve is also the one that generally provides the highest cooling power. The only exception is the set of tests done at a condenser temperature of 25 °C, which shows a monotonically decreasing trend. This behavior differs from the other curves, which exhibit a well-defined efficiency peak. We believe that, in this case, the maximum EER likely occurs at a valve opening lower than 10 % — a region not explored in our tests — which could explain the absence of a visible peak. Additionally, the pressure trend in Fig. 4a for this same temperature shows slightly larger variations, which are mostly attributable to experimental uncertainty and are not observed at higher condensation temperatures, where the influence of valve closure becomes less significant.

Fig. 4 resumes the metrics that are more focused on targeting the HC-290 refrigeration cycle performances: condensation pressure, compression ratio, and isentropic efficiency.

The condensation pressure (Fig. 4a) is rather insensitive to the degree of lamination, especially at the higher temperature levels of 31 °C and 33 °C. Instead, a slightly larger reduction of the condensation pressure is observed at lower temperatures as the valve closes, likely due to the additional pressure losses introduced by the higher degree of lamination.

Predictably, the condensation pressure increases significantly, from 9 to 11 bar, as the condensation temperature rises from 25 °C to 33 °C.

The compression ratio as a function of the expansion valve aperture (Fig. 4b) reveals a well-defined operational region between 60 and 85 %, where its values vary from 1.5 to 1.65 as the condensation temperature increases from 25 °C to 33 °C. This range corresponds to the same optimal control range of the micro-HP as previously identified in Fig. 3a. Beyond this field, at higher degrees of throttling, the compression ratio increases significantly across all condensation temperature scenarios, following a similar linear trend. The interplay between the reduction in condensation pressure and the increase in compression ratio decreases evaporation pressure as the valve operates between 40 and 70 %. The isentropic efficiency of the miniaturized compressor is plotted in Fig. 4c. Overall, the efficiency is relatively low compared to standard, larger compressors typically used in conventional vapor compression systems. The values ranged between 0.2 and 0.4 while typically in larger compressors exploiting scroll or rotary technologies, the isentropic efficiency is between 0.5 and 0.9 [64–68]. Additionally, a general decreasing trend in isentropic efficiency is found as the throttling level increases, directly linked to the rising compression ratio (though few curves show some outliers).

The data resumed in Table 7 and Figs. 3 and 4 refer to the steady state regime of the micro HP (running continuously and steadily under constant working parameters). They provide valuable insight into analyzing the CV cycle for different operative conditions and ranking the appliance's performance compared to other commercially available products. However, they do not explain the system's behavior during the four transient phases described in Section 3.1.

A thorough analysis of the data for all 27 tests has highlighted that the time profiles of the measured parameters have a shape that is not specific to a single experiment. They are qualitatively consistent across all the tests related to case #1 (e.g., the shape of the trends is similar to each other). For this reason, for the sake of conciseness, it has been decided to focus the analysis and discussion on one experiment (the most representative for using the micro HP in a PECS). Specifically, the "static test" number #9 of Table 2 (rpm = 2110, lamination = 80 %; T_{eva} = 20 °C, T_{cond} = 28 °C, condenser configuration #1) was chosen.

Figu. 5e and f present the trend of the cooling (Φ_{eva}), heating (Φ_{cond}) and absorbed electric power versus time for the four phases. Focusing on the steady-state operation period, it is possible to see that the prototype achieves a cooling capacity of approximately: $\Phi_{eva} \approx 200$ W with 50 W of electric power consumption (including compressor power and auxiliaries like water circulation pumps and DAQ equipment).

This resulted in an EER fluctuating between 4 and 5 over the 20 min steady-state period.

Several valuable information come out from the transient phases shown in Fig. 5:

Table 7
Results of static tests with condenser configuration # 1, varying condensation temperature and lamination level. Fixed evaporator temperature at nominal 20°C.

#	T_1 °C	T_2 °C	T_3 °C	T_4 °C	T_5 °C	T_6 °C	T_7 °C	T_8 °C	p_1 bar_g	p_2 bar_g	p_3 bar_g	p_4 bar_g	Δ_{surr} °C	Δ_{sub} °C	η_{iso} -	Φ_{cond} W	Φ_{eva} W	P_{el} W	EER -	$\overline{T}_{eva}$ °C	$\overline{T}_{cond}$ [°C]	β -	Δh_{comp} kJ/kg	$\dot{m}_{HC-290}$ g/s
1	14.3	42.8	28.3	14.3	25.9	27.6	19.7	18.3	6.14	9.32	9.27	6.14	0.2	0.3	0.31	340	243	42	5.8	19.0	26.7	1.52	121.9	0.34
2	16.2	52.1	29.3	14.6	27.1	28.8	19.1	17.9	6.22	9.61	9.55	6.22	1.7	0.2	0.31	326	207	48	4.3	18.5	27.9	1.55	57.9	0.82
3	19.7	58.9	27.9	13.4	25.9	27.5	19.5	18.3	5.95	9.25	9.24	5.97	6.6	0.1	0.29	308	207	49	4.2	18.9	26.7	1.55	65.2	0.74
4	20.1	69.1	27.5	11.8	25.6	27.1	19.8	18.7	5.68	9.04	9.11	5.71	8.4	0.1	0.23	287	175	54	3.3	19.3	26.3	1.59	84.7	0.62
5	20.4	71.9	27.2	10.4	25.2	26.7	19.9	18.9	5.4	8.99	9	5.42	10.1	0.2	0.25	285	175	58	3.0	19.4	26.0	1.66	89.0	0.64
6	20.0	77.0	27.4	7.4	25.3	26.8	19.8	18.8	4.94	9.01	9.09	4.93	12.5	0.2	0.27	295	192	71	2.7	19.3	26.0	1.82	98.2	0.71
7	20.1	77.3	26.8	9.3	25.0	26.4	19.9	19.0	5.21	8.92	8.95	5.19	11.0	0	0.23	266	160	67	2.4	19.4	25.7	1.71	99.8	0.66
8	15.1	45.9	30.2	15.2	28.3	29.6	19.8	18.7	6.34	9.81	9.76	6.35	0	0.3	0.13	310	188	54	3.5	19.2	28.9	1.55	282.1	0.19
9	17.8	52.4	30.0	15.8	27.8	29.4	19.9	18.7	6.45	9.68	9.7	6.48	2.1	0.3	0.3	306	199	44	4.5	19.3	28.6	1.50	56.3	0.77
10	20.0	61.6	29.5	14.3	27.5	29.0	19.8	18.8	6.12	9.62	9.63	6.14	6	0.1	0.28	296	184	57	3.2	19.3	28.3	1.57	69.7	0.80
11	20.4	72.9	29.5	12.9	27.5	29.0	20.0	19.0	5.87	9.59	9.6	5.92	7.7	0.2	0.23	279	174	61	2.9	19.5	28.3	1.63	91.2	0.65
12	19.9	79.8	29.3	12.1	27.5	28.9	19.4	18.6	5.74	9.54	9.52	5.74	7.8	0.3	0.2	254	142	67	2.1	19.0	28.2	1.66	106.2	0.62
13	20.6	82.7	29.2	12.0	27.6	28.8	19.9	19.2	5.68	9.5	9.54	5.73	8.9	0.2	0.2	240	133	72	1.8	19.5	28.2	1.67	110.6	0.64
14	20.1	87.2	29.2	11.7	27.6	28.8	19.7	19.0	5.64	9.46	9.5	5.67	8.6	0.3	0.18	234	120	70	1.7	19.3	28.2	1.68	120.8	0.57
15	16.5	46.5	32.2	16.5	30.3	31.6	19.7	19.0	6.55	10.4	10.3	6.64	0.3	0.4	0.38	248	119	70	1.7	19.3	31.0	1.58	83.7	0.82
16	16.2	53.6	32.3	16.1	30.3	31.8	19.9	18.9	6.5	10.4	10.4	6.53	0.3	0.3	0.29	283	165	60	2.7	19.4	31.1	1.60	98.7	0.60
17	20.0	66.8	32.2	15.8	30.4	31.8	19.9	18.9	6.48	10.3	10.4	6.53	4.2	0.1	0.25	277	166	66	2.5	19.4	31.1	1.59	79.9	0.80
18	20.7	79.8	32.2	14.8	30.4	31.8	20.4	19.5	6.27	10.3	10.3	6.28	5.9	0.2	0.2	265	149	78	1.9	19.9	31.1	1.64	104.9	0.73
19	20.7	87.4	32.1	13.9	30.4	31.7	20.3	19.6	6.09	10.3	10.3	6.07	6.9	0.2	0.19	246	131	82	1.6	19.9	31.0	1.69	120.1	0.67
20	20.4	90.3	32.0	14.0	30.4	31.6	20.0	19.3	6.08	10.2	10.3	6.09	6.6	0.2	0.18	231	116	83	1.4	19.7	31.0	1.68	126.8	0.64
21	20.2	97.8	31.9	13.3	30.4	31.7	19.7	19.1	5.95	10.3	10.3	5.95	7.1	0.1	0.16	236	103	94	1.1	19.4	31.0	1.72	142.5	0.64
22	16.6	51.5	34.2	16.7	32.2	33.7	19.9	19.2	6.64	10.9	10.8	6.66	-0.1	0.5	0.26	274	124	94	1.3	19.6	32.9	1.65	170.2	0.54
23	16.8	52.9	34.2	17.1	32.3	33.6	19.9	19.2	6.68	10.9	10.8	6.7	0	0.5	0.21	255	123	75	1.6	19.6	32.9	1.63	211.7	0.35
24	18.9	72.3	34.0	16.6	32.3	33.7	19.7	18.9	6.57	10.8	10.8	6.61	2.7	0.3	0.23	293	138	78	1.8	19.3	33.0	1.65	92.4	0.82
25	20.0	84.9	34.2	13.8	32.2	33.7	19.6	18.7	6.04	10.8	10.8	6.06	6.4	0.3	0.22	299	145	95	1.5	19.1	33.0	1.79	114.7	0.81
26	20.1	93.7	34.1	12.5	32.2	33.7	19.7	18.9	5.8	10.8	10.9	5.82	7.8	0.1	0.2	291	142	104	1.4	19.3	33.0	1.87	132.2	0.77
27	20.3	86.7	33.6	14.0	32.1	33.3	19.6	19.0	6.07	10.8	10.8	6.06	6.5	-0.1	0.21	221	106	98	1.1	19.3	32.7	1.77	118.1	0.81

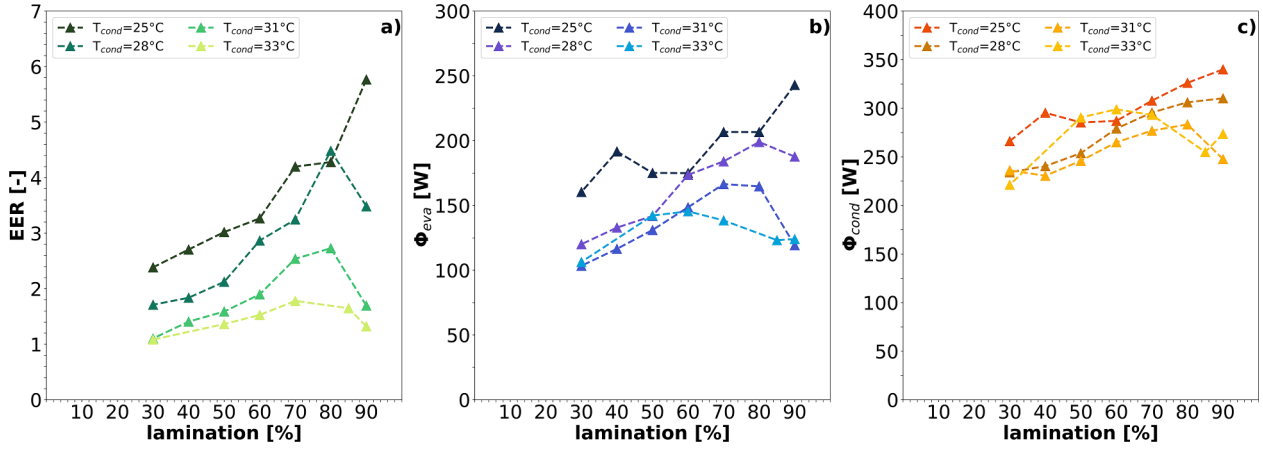

Fig. 3. Maps of heat pump functioning under conditions similar to the application of the PECS.

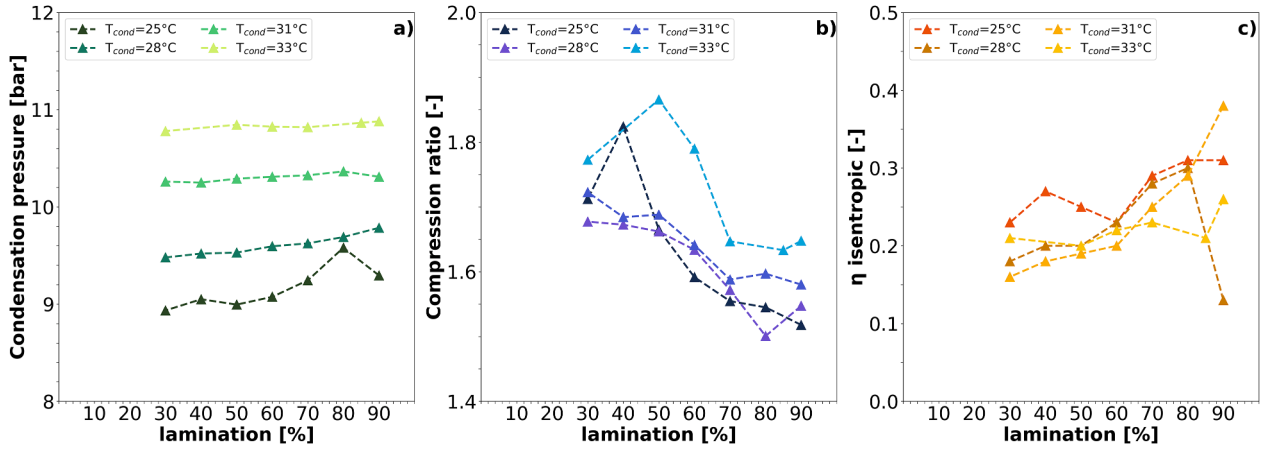

Fig. 4. Maps of the heat pump performance parameters under different conditions of functioning.

- *Refrigerant pressure*: pressure drops across the HC-290/water plate heat exchanger are negligible compared to those caused by the lamination valve. As seen in Fig. 5b, pressures remain nearly equal on either side of both exchangers ($p_2 \approx p_3$ and $p_4 \approx p_1$), with pressure differences across the evaporator and condenser measured at approximately $\Delta p_{eva} \approx \Delta p_{cond} = 2$ - 5 kPa. Meanwhile, the differential pressure between the evaporator and condenser remains around 4-5 bar in this specific test, while in other tests this difference is between 6-7 bar (summarized results in Table 6).
- *Power absorption*: the system exhibits an initial surge in power consumption immediately after the compressor starts, but stabilizes within a few minutes as the compressor speed reaches steady-state (Fig. 5d). The resistance forces opposing refrigerant mass flow in the PECS circuit primarily induce the compressor electrical draw. These resistance forces are influenced by two factors: the aperture of the expansion valve orifice and the refrigerant velocity, which is proportional to the rotational speed of the twin rotary compressor. Since both parameters (rpm and % of aperture of the lamination valve) remain constant during each test, power consumption stabilizes accordingly. Additionally, auxiliary current drawn by the auxiliaries is minimal/negligible (< 0.1 A).
- *HC-290 temperatures*:
  - a slight oscillation of the temperature in the evaporator is observed during the stationary phase, mostly due to the hysteresis of the thermostatic control used to keep a fixed setpoint water temperature (~20 °C in these tests, Fig. 5c). In the experiments, the cooling load is simulated using an electric heater, which regulates the water temperature at the evaporator. This heater operates with an on/off control logic: it turns on when the $T_{water} < T_{set\text{-}point} - \Delta T_{hystersis}$ and off when $T_{water} > T_{set\text{-}point} + \Delta T_{hystersis}$. As a result, the water temperature fluctuates by approximately $\pm\Delta T_{hystersis}$ around the setpoint, leading to an oscillation of $\sim 2\Delta T_{hystersis}$ (visible in Fig. 5c). In this setup, $\Delta T_{hysteresis}$ was set to 0.5 °C. In the longer steady-state phase, these variations are not producing any noteworthy inaccuracy, because the large number of data collected (>100) ensures a statistically significant mean value.
  - the refrigerant temperatures at the inlet of the compressor and of the evaporator requires a longer time to stabilize and to reach a consistent steady-state value (about 10 min). On the contrary, the temperatures at the outlet of the condenser and of the evaporator reach the steady state value after a few tens of seconds.
- *Instantaneous performance:* even during the *transient phase*, instantaneous performance metrics - such as heat exchange rates and power consumption (Fig. 5e) and instantaneous EER (Fig. 5f) - can be evaluated. These metrics represent the average system's performance within 15-second intervals, corresponding to the DAQ sampling time and averaging period.
- Finally, the *phase-down* period shows analogous features for all the tests. This final phase begins when the compressor is switched off and lasts until the test concludes. During this period, KPI metrics (e.g., heat exchange, power consumption, and EER) are no longer valid, as the micro-HP is no longer active. However, water circulation remains operational, and refrigerant and water temperatures and pressures return quickly to their initial conditions.

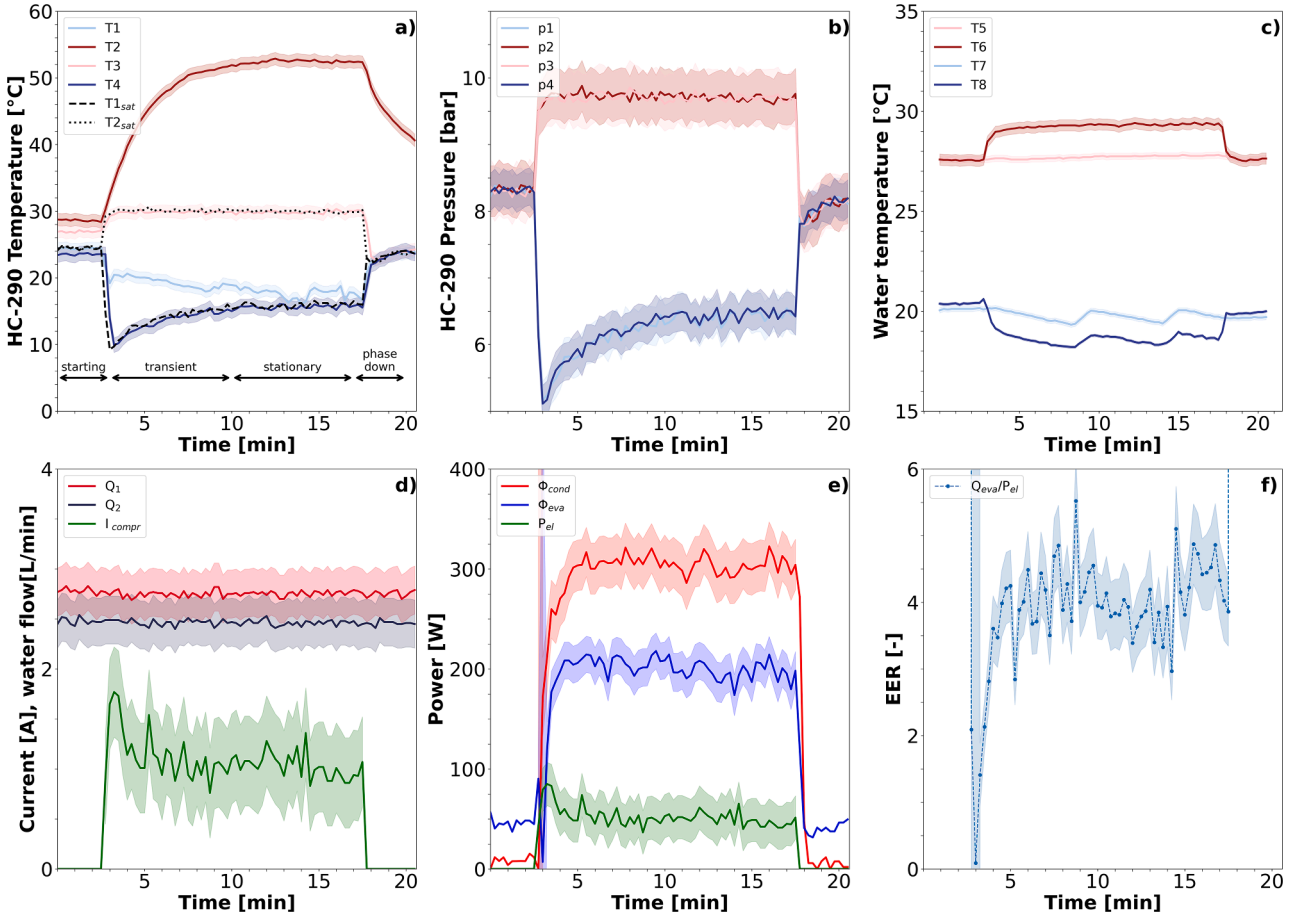

Fig. 5. Test #9 - Example of test coupling the micro-HP with the thermostatic bath at the condenser and evaporator.

4.2. Performance for typical PECS applications with the storage of the rejected heat

An additional experimental campaign was conducted in relation to cases where the rejected heat is stored and the condensing temperature is not fully controlled and may vary over time.

In this scenario, the appliance works in dynamically variable conditions and cannot operate continuously and indefinitely, but only for a certain period. When the temperature of the refrigerant at the outlet of the compressor exceeds certain limits, the compressor must be switched off to avoid damage (such temperature, in turn, corresponds to a certain condensing temperature).

Therefore, the first important information that can be derived from these experiments is the time period over which the PECS can operate before stopping.

A PECS is inherently designed to be used only where and when it is needed. Therefore, it is consistent to imagine that in a real application, it is required to work for a time shorter than the occupied period (typically 8 hours for an office building). On the other hand, it must also provide an operative time reasonably long, which may be estimated at no less than 4 to 6 hours.

The first explored configuration (case #2) adopts a TES based on water, while the second (case #3) uses an LHTES.

4.2.1. Performances with a water-based TES (case #2)

A total of 13 tests were done, keeping constant the aperture of the lamination valve and varying: the refrigerant charge, the compressor rpm, the initial temperature and the volume of the TES (5 l and 20 l. Table 3). Table 8 summarizes the relevant quantities measured during these tests (as arithmetic average over each testing period) and the corresponding performance of the prototype (EER, Φ_{eva}, Φ_{cond}). The same table shows also the maximum cooling capacity and the total stored heat.

Table 9 resumes, for the tests using the same amount of HC-290 mass in the refrigerant loop, the duration of the working time of the micro HP and the refrigerant temperature at the outlet of the compressor (the highest point in the loop) corresponding to the moment when condensation temperature reached about 36 °C. The first tests are not included in this comparison because of the different refrigerant mass in the circuit, and also for the limited size of the TES. In the end tests from #29 to #36 generated a useful effect only for a limited period of time (much less than the test duration that was around 0,5 h).

As it is possible to see, using a 20 l TES (that is already quite big for a stand-alone and moveable application) the maximum operative time was about 2 h (test #36, 38 and 40) and it frequently went down to 30-50 min. Such durations are not sufficient to satisfy the typical requirements for an adequate use of PECS. Moreover, in many of this tests the EER is below the unit, demonstrating a limited feasibility for a real application.

In order to analyze more in detail the behavior of the prototype with the TES, the experiment #38 was selected. Fig. 6 shows the corresponding trends of the relevant quantities versus time.

During the measurements, the cooling load was simulated using the same arrangement described in Section 4.1. The condenser, unlike configuration #1, is not thermally controlled since it is coupled to a sensible thermal energy storage. Hence, the condensing temperature starts from a certain initial value (20 °C, 22 °C and 27 °C, depending on the test, see Table 3) and then rises gradually. Such features strongly influenced the performance of the micro HP.

Fig. 6a shows that with a 20 l TES the capacity of heat rejection was

Table 8
Results of dynamic tests with TES (config. #2) and LHTES (config. #3), varying condensation temperature and lamination level. Fixed evaporator temp. at nominal 20°C.

#		T_1	T_2	T_3	T_4	T_5	T_6	T_7	T_8	p_1	p_2	p_3	p_4	Δ_{surr}	Δ_{sub}	Φ_{cond}	Φ_{eva}	P_{el}	EER	$\bar{T}_{eva}$	$\bar{T}_{cond}$	β	Duration	Stored Heat	Cooling Capacity
		°C	°C	°C	°C	°C	°C	°C	°C	bar_g	bar_g	bar_g	bar_g	°C	°C	W	W	W	-	°C	[°C]	-	hours	kWh	kWh
TES	**29**	19.2	51.7	39.3	18.8	38.9	43.7	21.5	20.7	7.1	15.3	15.3	7.1	0.42	8.42	316	169	227	0.78	21.1	41.3	2.2	0.5	0.16	0.08
	30	18.5	59.4	39.1	17.3	38.5	44.3	21.3	20.1	6.8	16.4	16.5	6.8	1.1	11.9	377	237	282	0.75	20.7	41.4	2.4	0.5	0.19	0.12
	31	19.3	63.9	43.1	18.6	42.2	47.9	21.6	20.7	7.0	17.7	17.7	7.0	1.4	13	402	210	349	0.8	21.2	45.1	2.5	0.5	0.20	0.11
	32	18.8	66.5	41.1	17.3	30.2	46.6	21.4	19.8	6.8	17.7	17.7	6.8	1.4	13	452	319	342	0.6	20.6	43.3	2.6	0.5	0.23	0.17
	33	16	43.2	29.7	15.2	29.3	34.6	19.3	17.9	6.3	12.3	12.4	6.3	1.1	9.4	360	240	118	2.0	18.6	31.9	2.0	1	0.37	0.25
	34	20.3	56.4	31.9	19.3	31.4	38.6	25.7	23.5	7.2	14.9	15.0	7.2	1.1	15	474	415	167	2.5	24.6	35	2.1	0.5	0.21	0.18
	35	22.5	41.1	32.2	21.7	31.8	36.4	25.8	24.2	7.7	12.3	12.3	7.7	1.0	6.5	307	283	65.1	4.4	25.0	34.1	1.6	0.67	0.20	0.19
	36	16.9	34.9	32.1	16.5	30	32.8	18.2	17.8	6.6	10.8	10.8	6.6	0.49	1.58	187	75	57	1.3	18.0	31.4	1.6	2.25	0.43	0.17
	37	19.3	100	31.2	3.5	28.5	30.8	19.1	17.4	4.2	10.1	10.1	4.3	16.3	0	424	301	177	1.7	18.2	29.6	2.4	0.83	0.35	0.25
	38	19.6	77.8	30	12.8	28.5	29.6	19.4	18.8	5.9	9.8	9.8	5.9	6.7	0	221	121	64	1.9	19.1	29.1	1.7	2	0.43	0.23
	39	26	77.1	33.4	14.6	31.4	32.8	26.5	25.3	6.2	10.7	10.7	6.2	11.6	0	270	221	78	2.8	25.9	32.1	1.8	0.83	0.22	0.18
	40	20	82.1	29.7	11.0	28.1	29.3	19.8	18.9	5.5	9.7	9.7	5.6	9.3	0	233	157	69.2	2.3	19.4	28.7	1.8	1.83	0.41	0.28
	41	26.1	84.2	33.3	13.5	31.5	32.9	26.7	25.3	6.0	10.7	10.7	6.0	12.7	0	254	252	85	3.0	26.0	32.2	1.8	0.83	0.20	0.20
LHTES	**42**	24.2	100	39.1	19.6	36.9	38.8	24.4	23.7	7.3	12.4	12.4	7.3	4.5	0	238	138	111	1.2	24.1	37.9	1.7	5	1.13	0.65
	43	24.2	90.7	35.6	16.2	33.3	35.3	24.4	23.4	6.5	11.5	11.6	6.5	8.3	0.8	293	181	92	2.0	23.9	34.3	1.7	8	2.58	1.60
	44	24.2	87.3	34.8	16.2	32.5	34.6	24.4	23.4	6.5	11.1	11.1	6.5	8.3	0	306	188	86	2.2	23.9	33.5	1.7	8	3.10	1.90
	45	24.1	76.1	30.9	13.4	28.3	30.5	24.3	23.0	5.9	10.0	10.0	6.0	11	0	318	233	68	3.4	23.7	29.4	1.7	8	2.60	1.90

Table 9
Results of dynamic tests with TES (config. #2) maximum duration of the working period and final temperature of the refrigerant at the compressor outlet.

#		Duration hours	Max temperature °C
TES	**37**	0,83	125,0
	38	2	104,8
	39	0,83	91,1
	40	1,83	111,0
	41	0,83	99,6
LHTES	**42**	5	115,0
	43	8	94,4
	44	8	91,7
	45	8	78,4

limited, and could sustain the operations for less than two hours. As a result, the compressor outlet temperature (T_2) of the HC-290 refrigerant gradually increased, approaching the maximum allowable limit of 110°C. Upon reaching this threshold, the compressor's safety controls automatically shut down the unit to prevent overheating. In fact, beyond 115 °C, lubricant degradation and damage to sealing components put the component at significant risk.

As heat accumulated within the TES, the condenser pressure (p_2) steadily rose from about 7 bar to approximately 12 bar (Fig. 6b), while the evaporator pressure (p_1) remained relatively stable at around 5 bar in the initial phase, but eventually increased to 7 bar. Consequently, the evaporator outlet temperature of HC-290 also rose, reducing the achievable value of the TCC.

Since this storage system operates solely through sensible heat rejection, the water temperature increased continuously over time (Fig. 6c), progressively diminishing the effectiveness of the process. In less than two hours, the water temperature rose from 20 °C to 36 °C, further limiting the system's ability to absorb and dissipate heat efficiently.

4.2.2. *Performances with a LHTES based on PCM (case #3)*

As far as the performance of the LHTES configuration (#3) are concerned, the presence of a PCM significantly enhanced: the heat storage capacity of the rejection tank, and the stabilization of the temperatures of the HC-290/water and of the pressures of the refrigerant. A better control and stability of the condensation temperature/pressure positively impacted the overall operation of the micro-HP. Unlike configuration #2 (TES, see e.g. Fig. 6), where a *stationary phase* was never reached, the test results plotted in Fig. 7 demonstrate an extended period of stationary operation, following the initial *transient phase*. Fig. 7 refers, as an example, to test #43.

It is worth noting, however, that unlike the steady-state results observed in case #1 (Section 4.1), the initial transient phase in these tests is not associated with the complete stabilization of the compressor working parameters. About 2 h are needed (Fig. 7a, b) to reach a full stabilization of the pressures and temperatures at the inlet and outlet of the compressor (while for config. # 1 few minutes were enough to attain a steady-state). This is due to the mechanism of the heat storage in the LHTES. At the beginning the heat is stored within the solid PCM in a sensible way; the temperature, therefore, keeps rising (see e.g. T_3 – pink curve – in Fig. 7a), starting from its initial value up to melting temperature, when the phase transition occurs at approximately 33 °C (Fig. 7a and b).

Once the transition from the solid to the slurry phase begins (after about 2 h), the temperature profile stabilizes, reaching a quasi-steady-state operation that persists as long as the PCM continues its solid-to-liquid phase change. The temperature of the water circulating through the plate heat exchanger at the condenser follows a similar trend, gradually increasing and stabilizing at around 34 – 36 °C over the same 120 min period.

Notably, the system was able to be fully operational and stable for

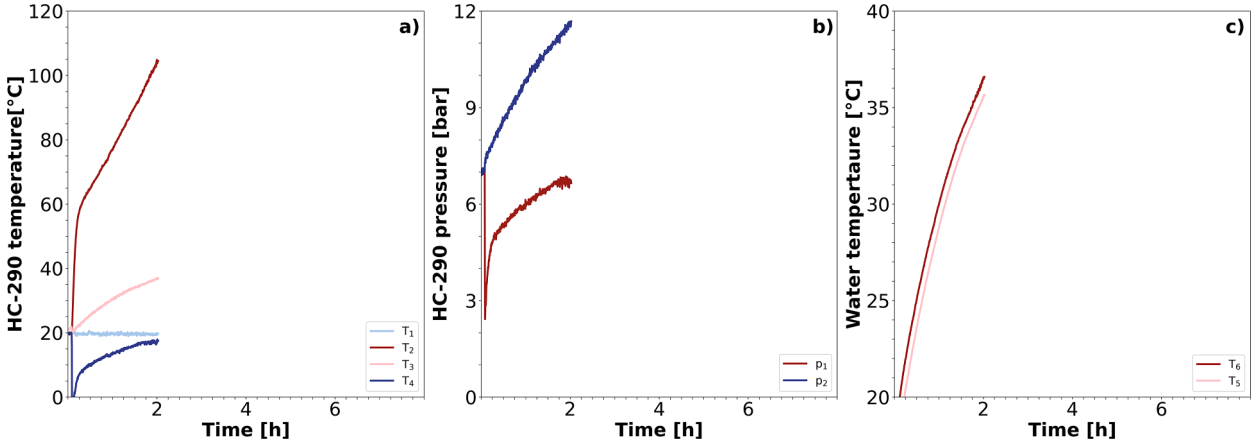

Fig. 6. Test #38, Time series of HC-290 temperature (a) and pressure (b) during a test with rejection heat in configuration #2. In (c) the time series of the inlet and outlet water from the plate heat exchanger at the condenser.

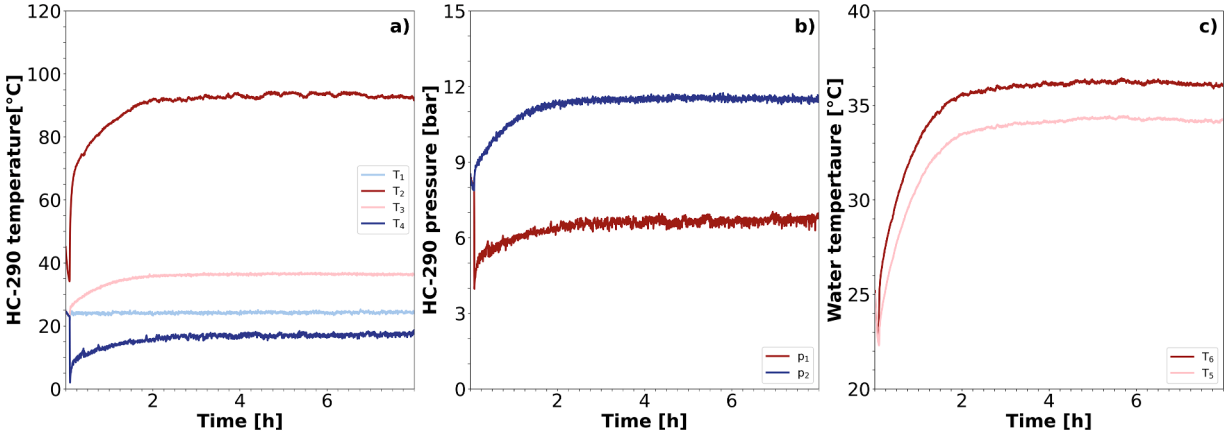

Fig. 7. Test #43, Time series of HC-290 temperature (a) and pressure (b) during a test with rejection heat in configuration #3. In (c) the time series of the inlet and outlet water from the plate heat exchanger at the condenser.

about eight hours in this test, as well as in all other tests conducted under configuration #3, as summarized in Table 8.

4.2.3. *Comparison of performance between TES – LHTES configurations*

In order to compare the performance of the micro HP working with different condenser configurations, two tests done under similar boundary and operational conditions were selected, that is, test #38 for case #2 and #43 for case #3.

Fig. 8 shows in order: the dynamic time trend of the heat exchanged at the evaporator for test #38 (8a) and for test #43 (8b), the

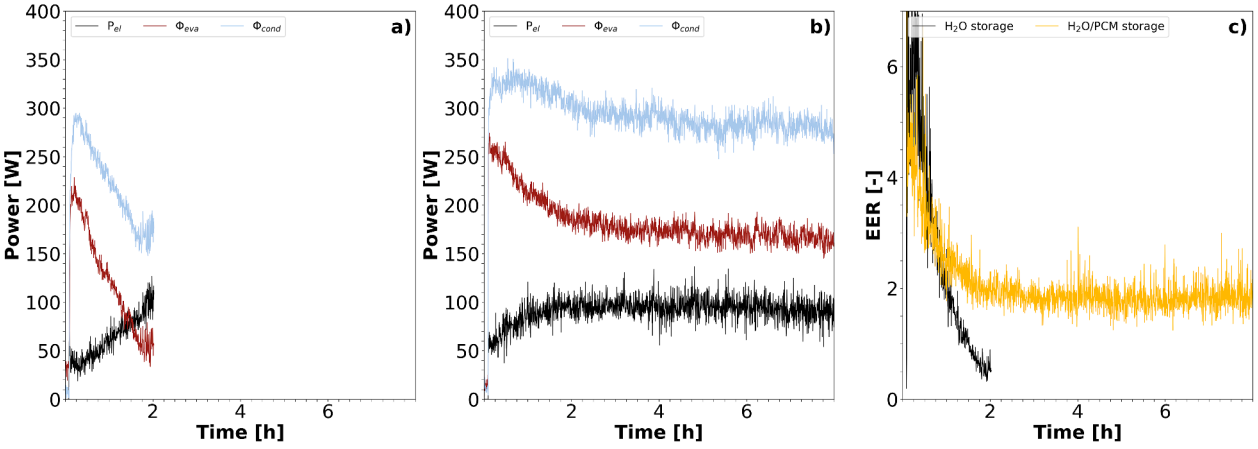

Fig. 8. In (a), the trend of the system's exchanged heat (red and blue) and the electric power consumptions (black) of the micro-HP in the case #2 with the water-based TES. In (b), the same comparison is done for heat rejection in the case #3 using the the PCM/water LHTES. In (c), the comparison between the two configurations based on the EER.

instantaneous trend of the EER (8c). The heat exchange rate at the evaporator was initially rather similar in both cases — 200 W for case #2 (Fig. 8a) and 250 W for case #3 (Fig. 8b). However, in case #2, the cooling capacity steadily declined over time, dropping below 50 W after approximately 120 min. In contrast, case #3 exhibited an initial transient phase due to the accumulation of the PCM's sensible heat in the LHTES storage. After this phase, the cooling capacity stabilized at around 180 W. Similarly, the power absorbed by the system increased from 50 W to 100 W and remained stable at this level for more than six hours.

Operations using the LHTES system resulted in an EER ranging between 2 and 4 (Fig. 8c). Although the average EER was similar for both configurations — approximately 2 — the total energy exchanged was significantly higher in the latent heat configuration. Specifically, it provided 1.6 kWh of cooling while consuming 0.8 kWh of electricity and rejecting 2.6 kWh of total heat.

Most of the rejected heat was absorbed into the storage tank. However, increased turbulence caused by the mechanical stirrer led to higher heat losses to the environment. Despite this, the mechanical stirrer was essential during this prototypal phase due to the low thermal conductivity and density of PCM compared to water. Without vigorous mixing, thermal exchange would have been significantly reduced, compromising system performance. Notably, the cold water at the evaporator outlet remained below 15 °C throughout all experiments, ensuring a sufficiently low temperature to provide effective individual cooling during summer conditions.

5. Conclusions

The experimental results highlighted that the performance of this micro-HP prototype were suitable for a PECS application. By leveraging the latent heat of PCM, the micro-HP demonstrated improved stability in rejection tank temperatures, mitigating operational risks, such as excessive HC-290 outlet temperatures and high condenser pressures. The micro-HP coupled with the LHTES operated with a EER between 2 and 4, despite the isentropic efficiencies ranged only between 0.2 and 0.4 (values that are significantly lower than typical scroll or rotary compressors). Although the average EER was similar between the two storages (the TES and the LHTES) and close to 2, the total energy exchanged was much higher in the LHTES. It produced 1.6 kWh of cooling, absorbing 0.8 kWh of electricity, and rejecting 2.6 kWh of total heat. This was obtained with an operational time that ranged from 5 to 8 h. When compared to other miniaturized active cooling technologies suitable for PECS, the proposed system demonstrated superior energy performance and a cooling capacity that exceeds the typical requirements for personal thermal comfort.

The latent heat storage not only extends operational duration but also supports more consistent cooling performance with reduced environmental heat losses, especially with the inclusion of a mechanical stirrer to address the low thermal conductivity of PCM. While the mechanical stirrer introduces additional complexity, its use was crucial in this prototypal phase to ensure an effective heat transfer. Future developments should aim to optimize the heat exchange between the HC-290 and the phase change material and the PCM formulations. This optimization will allow to eliminate the mechanical stirring in the storage tank.

The designed prototype exploited plate water/refrigerant heat exchangers to facilitate accurate thermal power measurements by leveraging the incompressible nature of water, simplifying monitoring and ensuring stable testing conditions. However, this approach introduced additional heat exchanges that are not strictly necessary in both the evaporation and condensation sides. Substituting the heat exchangers of the cooling side with a direct air/refrigerant exchange is preferable in real environmental applications. This approach enables direct thermal interaction with the occupant without relying on intermediate fluid flows, reducing system complexity, improving responsiveness and thermal exchange efficiency.

On the condenser side, a heat exchanger configuration is preferred that would directly incorporate PCM, exploiting a direct contact between the metal surface and the materials. This adjustment, eliminating again the intermediate water flow, results in thermal effectiveness enhancement of the heat rejection during condensation. Finally, contributing to higher EER values.

Another potential improvement to enhance the cooling cycle's performance involves optimizing the compressor's thermal management. By configuring the system so that a small fan directs airflow from the surrounding environment onto the compressor casing, excess heat can be dissipated more effectively. Cooling the compressor's outer shell improves its η_{iso} leading to a higher overall EER. Additionally, it helps lowering the outlet temperature (T_2), which in turn reduces the thermal load on the LHTES system, potentially allowing for a more compact storage design. In addition, in future studies, given the possibility to control the lowest temperature of the cooling cycle, we will explore also the impact on comfort when acting not only on temperature and air velocity, but also on relative humidity.

Despite the promising performance of the proposed micro-HP system, the large-scale deployment of PECS in real buildings still faces several barriers. First, the lack of standardized components for personal-scale heat pumps complicates design efforts and limits availability. Second, the use of flammable refrigerants, although minimal in quantity, requires compliance with evolving safety regulations, particularly in indoor environments. Third, the need to manage the rejected heat remains a fundamental issue; in this work, we propose onboard thermal energy storage as a strategy to decouple cooling operation and heat release, potentially avoiding the need for ducting. Moreover, user acceptance and ergonomic integration within workspace furniture—considering acoustics, control interfaces, and aesthetic impact—are essential for real-world adoption. Finally, while this prototype remains pre-commercial, its reliance on scalable and widely available components (e.g., miniature rotary compressors used in domestic appliances) suggests that future cost reductions and industrial scalability are plausible. These aspects will need to be addressed in future research phases through interdisciplinary collaborations and pilot studies in real-world environments.

CRediT authorship contribution statement

V. Gentile: Writing – review & editing, Writing – original draft, Visualization, Validation, Methodology, Investigation, Data curation, Conceptualization. **M. Perino:** Writing – review & editing, Writing – original draft, Methodology, Funding acquisition, Conceptualization.

Declaration of competing interest

We confirm that the manuscript has been read and approved by all named authors and that there are no other persons who satisfied the criteria for authorship but are not listed. We further confirm that all have approved the order of authors listed in the manuscript.

We confirm that we have given due consideration to the protection of intellectual property associated with this work and that there are no impediments to publication, including the timing of publication, concerning intellectual property. In so doing, we confirm that we have followed the regulations of our institutions concerning intellectual property.

The authors Vincenzo Gentile and Marco Perino reports financial support from a project funded under the National Recovery and Resilience Plan (NRRP), Mission 4 Component 2 Investment 1.3 - Call for tender No. 1561 of 11.10.2022 of Ministero dell'Università e della Ricerca (MUR); funded by the European Union – NextGenerationEU. Award Number: Project code PE0000021, Concession Decree No. 1561 of 11.10.2022 adopted by Ministero dell'Università e della Ricerca (MUR), CUP E13C22001890001, according to attachment E of Decree

No. 1561/2022, Project title "Network 4 Energy Sustainable Transition – NEST".

We understand that the Corresponding Author is the sole contact for the Editorial process (including the Editorial Manager and direct communications with the office). He is responsible for communicating with the other authors about progress, submissions of revisions, and final approval of proofs. We confirm that we have provided a current, correct email address which is accessible by the Corresponding Author and which has been configured to accept email from *vincenzo.gentile@polito.it*

Acknowledgments

The research activity presented in this paper is done in a project funded under the National Recovery and Resilience Plan (NRRP), Mission 4 Component 2 Investment 1.3 - Call for tender No. 1561 of 11.10.2022 of Ministero dell'Università e della Ricerca (MUR); funded by the European Union – NextGenerationEU. Award Number: Project code PE0000021, Concession Decree No. 1561 of 11.10.2022 adopted by Ministero dell'Università e della Ricerca (MUR), CUP E13C22001890001, according to attachment E of Decree No. 1561/2022, Project title "Network 4 Energy Sustainable Transition – NEST".

Data availability

Data will be made available on request.

References

[1] "IEA EBC Annex87 - Energy and indoor environmental quality performance of personalised environmental control systems. Accessed: March 11, 2025." https://annex87.iea-ebc.org/(accessed Mar. 11, 2025).
[2] J. Ling, et al., Energy savings and thermal comfort evaluation of a novel personal conditioning device, Energy Build. 241 (2021) 110917, https://doi.org/10.1016/j.enbuild.2021.110917.
[3] Z. Nagy, et al., Ten questions concerning occupant-centric control and operations, Build. Environ. 242 (June) (2023), https://doi.org/10.1016/j.buildenv.2023.110518.
[4] M. André, R. De Vecchi, R. Lamberts, User-centered environmental control: a review of current findings on personal conditioning systems and personal comfort models, Energy Build. 222 (2020), https://doi.org/10.1016/j.enbuild.2020.110011.
[5] J. Kim, S. Schiavon, G. Brager, Personal comfort models – a new paradigm in thermal comfort for occupant-centric environmental control, Build. Environ. 132 (November 2017) (2018) 114–124, https://doi.org/10.1016/j.buildenv.2018.01.023.
[6] "European Committee for Standardization (CEN), "EN ISO 7730:2005 - Ergonomics of the thermal environment - analytical determination and interpretation of thermal comfort using calculation of the PMV and PPD indices and local thermal comfort criteria (ISO 7".
[7] S.P.A. Hedge, A. Michael, Reactions of facilities managers and office workers to underfloor task air ventilation, J. Arch. Plan. Res. 10 (1993) 203–218.
[8] M. Fountain, E. Arens, R. de Dear R, et al., Locally controlled air movement preferred in warm isothermal environments, ASHRAE Trans. 100 (2) (1994) 937–952.
[9] W.M. Kroner, Environmentally responsive workstations and office worker productivity, ASHRAE Trans. 100 (2) (1994) 750–755.
[10] W.J. Fisk, "Health and productivity gains from better indoor environments and their implications for the US Department of Energy (No. LBNL-47458)," 2000.
[11] F. Bauman, A. Baughman, G. Carter, et al., A Field Study of PEM (Personal Environmental Module) Performance in Bank of America's San Francisco Office Buildings, Center for Environmental Design Research, 1997.
[12] "IEA - International Energy Agency, 'The future of cooling opportunities for energy-efficient air conditioning together. Accessed: Mar. 11, 2025 Secure sustainable.'" https://www.iea.org/reports/the-future-of-cooling.
[13] R. Rawal, M. Schweiker, O.B. Kazanci, V. Vardhan, Q. Jin, L. Duanmu, Personal comfort systems: a review on comfort, energy, and economics, Energy Build. 214 (2020), https://doi.org/10.1016/j.enbuild.2020.109858.
[14] J. Verhaart, M. Veselý, W. Zeiler, Personal heating: effectiveness and energy use, Build. Res. Inf. 43 (3) (2015) 346–354, https://doi.org/10.1080/09613218.2015.1001606.
[15] M. Veselý, W. Zeiler, Personalized conditioning and its impact on thermal comfort and energy performance - a review, Renew. Sustain. Energy Rev. 34 (2014) 401–408, https://doi.org/10.1016/j.rser.2014.03.024.
[16] S. Schiavon, A.K. Melikov, Energy saving and improved comfort by increased air movement, Energy Build. 40 (10) (2008) 1954–1960, https://doi.org/10.1016/j.enbuild.2008.05.001.
[17] A. Lipczynska, S. Schiavon, L.T. Graham, Thermal comfort and self-reported productivity in an office with ceiling fans in the tropics, Build. Environ. 135 (March) (2018) 202–212, https://doi.org/10.1016/j.buildenv.2018.03.013.
[18] Y. He, W. Chen, Z. Wang, H. Zhang, Review of fan-use rates in field studies and their effects on thermal comfort, energy conservation, and human productivity, Energy Build. 194 (2019) 140–162, https://doi.org/10.1016/j.enbuild.2019.04.015.
[19] M. Heidarinejad, D.A. Dalgo, N.W. Mattise, J. Srebric, Personalized cooling as an energy efficiency technology for city energy footprint reduction, J. Clean. Prod. 171 (2018) 491–505, https://doi.org/10.1016/j.jclepro.2017.10.008.
[20] W. Chakroun, N. Ghaddar, K. Ghali, Chilled ceiling and displacement ventilation aided with personalized evaporative cooler, Energy Build. 43 (11) (2011) 3250–3257, https://doi.org/10.1016/j.enbuild.2011.08.026.
[21] S. Schiavon, A.K. Melikov, C. Sekhar, Energy analysis of the personalized ventilation system in hot and humid climates, Energy Build. 42 (5) (2010) 699–707, https://doi.org/10.1016/j.enbuild.2009.11.009.
[22] T. Bauman, F. Arens, E.A. Fountain, M. Huizenga, C. Miura, K. Xu, T. Akimoto, T. Zhang, H. Faulkner, D. Fisk, W. Borgers, Localized Thermal distribution for office buildings; final report-phase III. UC Berkeley: Center for the Built Environment, 1994. Accessed: Mar. 112025, https://escholarship.org/uc/item/2pw6v7dz.
[23] H. Zhang, E. Arens, Y. Zhai, A review of the corrective power of personal comfort systems in non-neutral ambient environments, Build. Environ. 91 (2015) 15–41, https://doi.org/10.1016/j.buildenv.2015.03.013.
[24] M. Perino, M. Bilardo, E. Fabrizio, A framework for assessing the energy performance of Personalized Environmental Control Systems (PECS) for heating, cooling and ventilation, Build. Environ. 265 (July) (2024) 111925, https://doi.org/10.1016/j.buildenv.2024.111925.
[25] Y.F. Zhang, D.P. Wyon, L. Fang, A.K. Melikov, The influence of heated or cooled seats on the acceptable ambient temperature range, Ergonomics 50 (4) (2007) 586–600, https://doi.org/10.1080/00140130601154921.
[26] H. Zhang, E. Arens, D.E. Kim, E. Buchberger, F. Bauman, C. Huizenga, Comfort, perceived air quality, and work performance in a low-power task-ambient conditioning system, Build. Environ. 45 (1) (2010) 29–39, https://doi.org/10.1016/j.buildenv.2009.02.016.
[27] Z. Wilmer, P. Hui, Z. Ed, A. Soazig, K. Yongchao, Effect of a heated and cooled office chair on thermal comfort, HVAC&R Res. 19 (5) (2013) 574–583.
[28] W. Pasut, H. Zhang, E. Arens, Y. Zhai, Energy-efficient comfort with a heated/cooled chair: results from human subject tests, Build. Environ. 84 (2015) 10–21, https://doi.org/10.1016/j.buildenv.2014.10.026.
[29] H. Zhang, et al., Using footwarmers in offices for thermal comfort and energy savings, Energy Build. 104 (2015) 233–243, https://doi.org/10.1016/j.enbuild.2015.06.086.
[30] B. Yang, Z. Li, B. Zhou, T. Olofsson, A. Li, Enhanced effects of footwarmer by wearing sandals in winter office: a Swedish case study, Indoor Built Environ. 30 (7) (2021) 875–885, https://doi.org/10.1177/1420326X20913975.
[31] S. Atthajariyakul, C. Lertsatittanakorn, Small fan assisted air conditioner for thermal comfort and energy saving in Thailand, Energy Convers. Manag. 49 (10) (2008) 2499–2504, https://doi.org/10.1016/j.enconman.2008.05.028.
[32] S. Watanabe, A.K. Melikov, G.L. Knudsen, Design of an individually controlled system for an optimal thermal microenvironment, Build. Environ. 45 (3) (2010) 549–558, https://doi.org/10.1016/j.buildenv.2009.07.009.
[33] Y. Zhai, H. Zhang, Y. Zhang, W. Pasut, E. Arens, Q. Meng, Comfort under personally controlled air movement in warm and humid environments, Build. Environ. 65 (2013) 109–117, https://doi.org/10.1016/j.buildenv.2013.03.022.
[34] L. Huang, Q. Ouyang, Y. Zhu, L. Jiang, A study about the demand for air movement in warm environment, Build. Environ. 61 (2013) 27–33, https://doi.org/10.1016/j.buildenv.2012.12.002.
[35] S. Schiavon, B. Yang, Y. Donner, V.W.C. Chang, W.W. Nazaroff, Thermal comfort, perceived air quality, and cognitive performance when personally controlled air movement is used by tropically acclimatized persons, Indoor Air 27 (3) (2017) 690–702, https://doi.org/10.1111/ina.12352.
[36] M. He, H. Liu, L. Shao, B. Li, Y. Wu, Does back cooling improve human thermal comfort in warm environments? A device for heat conduction by the semiconductor Peltier effect, Build. Simul. 17 (8) (2024) 1253–1271, https://doi.org/10.1007/s12273-024-1139-0.
[37] A. Abdelmessih, et al., Personal heating/cooling system using peltier, in: ASME 2020 Int. Tech. Conf. Exhib. Packag. Integr. Electron. Photonic Microsystems, InterPACK 2020, 2020, pp. 1–11, https://doi.org/10.1115/IPACK2020-2625.
[38] H. Wei, J. Zhang, Y. Han, D. Xu, Soft-covered wearable thermoelectric device for body heat harvesting and on-skin cooling, Appl. Energy 326 (September) (2022) 119941, https://doi.org/10.1016/j.apenergy.2022.119941.
[39] B. Yang, X. Ding, F. Wang, A. Li, A review of intensified conditioning of personal micro-environments: moving closer to the human body, Energy Built Environ. 2 (3) (2021) 260–270, https://doi.org/10.1016/j.enbenv.2020.06.007.
[40] S.C. S, K.W.C.N. Gong, K.W. Tham, A.K. Melikov, D.P. Wyon, The acceptable air velocity range for local air movement in the tropics, HVAC&R Res. 12 (14) (2006) 1065–1076, https://doi.org/10.1080/10789669.2006.10391451.
[41] C.S.B. Yang, A. Melikov, Performance evaluation of ceiling mounted personalized ventilation system, ASHRAE Trans. 115 (2) (2009) 1065–1076.
[42] E.A. Arens, F.S. Bauman, L.P. Johnston, H. Zhang, Testing of localized ventilation systems in a new controlled environment chamber, Indoor Air 1 (3) (1991) 263–281, https://doi.org/10.1111/j.1600-0668.1991.05-13.x.
[43] P.O. Fanger, A.K. Melikov, H. Hanzawa, J. Ring, Air turbulence and sensation of draught, Energy Build. 12 (1) (1988) 21–39, https://doi.org/10.1016/0378-7788(88)90053-9.

[44] P.O. Fanger, Assessment of man's thermal comfort, ASHRAE Trans. 84 (1) (1978) 1–6.
[45] D.P.W. David Faulkner, W.J. Fisk, D.P. Sullivan, Ventilation efficiencies of desk-mounted task /ambient conditioning systems, Indoor Air 9 (4) (2004) 273–281.
[46] F.S. Bauman, L. Johnston, H. Zhang, Performance testing of a floor-based, occupant-controlled office ventilation system, ASHRAE Trans. 97 (1) (1991) 553–565.
[47] J. Shinoda, D.I. Bogatu, F. Watanabe, Y. Kaneko, B.W. Olesen, O.B. Kazanci, Performance evaluation of a multi-functional personalized environmental control system (PECS) prototype, Build. Environ. 252 (October 2023) (2024) 111260, https://doi.org/10.1016/j.buildenv.2024.111260.
[48] Dragos-Ioan Bogatu, Resilient cooling and ventilation for buildings and people, DTU - Technical University of Denmark, 2024.
[49] O.B. Kazanci, et al., Development and initial testing of a personalized environmental control system (PECS), in: *Proc. CLIMA 2022 Conf.*, no. May, 2022, pp. 49–56, https://doi.org/10.34641/clima.2022.239 [Online]Available:.
[50] D. Zhao, et al., Personal thermal management using portable thermoelectrics for potential building energy saving, Appl. Energy 218 (March) (2018) 282–291, https://doi.org/10.1016/j.apenergy.2018.02.158.
[51] F. Wang, et al., Cooling collars incorporated with PCM packs and gels to improve indoor thermal comfort in healthy young females, Build. Environ. 262 (June) (2024) 111788, https://doi.org/10.1016/j.buildenv.2024.111788.
[52] H. Xu, B. Cao, L. Gao, F. Wang, G. Jin, Z. Liu, Personal cooling garments with phase change material packages - a critical review of challenges, solutions and recent progress, Build. Environ. 250 (January) (2024) 111169, https://doi.org/10.1016/j.buildenv.2024.111169.
[53] W. Song, et al., Evaluating a novel portable semiconductor liquid cooling garment for reducing heat stress of healthcare workers in a hot-humid environment, Build. Environ. 267 (2024) 2025, https://doi.org/10.1016/j.buildenv.2024.112194.
[54] Y. Qiao, T. Cao, J. Muehlbauer, Y. Hwang, R. Radermacher, Experimental study of a personal cooling system integrated with phase change material, Appl. Therm. Eng. 170 (October 2019) (2020) 115026, https://doi.org/10.1016/j.applthermaleng.2020.115026.
[55] A.A. Al-Abidi, S. Bin Mat, K. Sopian, M.Y. Sulaiman, C.H. Lim, A. Th, Review of thermal energy storage for air conditioning systems, Renew. Sustain. Energy Rev. 16 (8) (2012) 5802–5819, https://doi.org/10.1016/j.rser.2012.05.030.
[56] C. Gao, K. Kuklane, F. Wang, I. Holmér, Personal cooling with phase change materials to improve thermal comfort from a heat wave perspective, Indoor Air 22 (6) (2012) 523–530, https://doi.org/10.1111/j.1600-0668.2012.00778.x.
[57] Y. Du, J. Muehlbauer, J. Ling, V. Aute, Y. Hwang, R. Radermacher, Rechargeable personal air conditioning device, in: ASME 2016 10th Int. Conf. Energy Sustain. ES2016, collocated with ASME 2016 Power Conf. ASME 2016 14th Int. Conf. Fuel Cell Sci. Eng. Technol. 1, 2016, pp. 1–5, https://doi.org/10.1115/ES2016-59253.
[58] R. Dhumane, Y. Du, J. Ling, V. Aute, R. Radermacher, M.H. Bldg, Transient modeling of a thermosiphon based air conditioner with compact thermal storage : modeling and validation, Int. Compress. Eng. Refrig. Air Cond. High Perform. Build. Conf. (Vcc) (2016) 1–10.
[59] T. E.P. and the council of E. Union, "REGULATION (EU) 2024/573 OF THE EUROPEAN PARLIAMENT AND OF THE COUNCIL of 7 February 2024 on fluorinated greenhouse gases, amending Directive (EU) 2019/1937 and repealing Regulation (EU) No 517/2014," 2024.
[60] BSIS Publication, "BS ISO 5149-1:2014+A2:2021, refrigerating systems and heat pumps — safety and environmental requirements," 2014.
[61] BS EN IEC 60335-2-89:2022+A11:2022, Household and similar electrical appliances — Safety for range hoods and other cooking. Particular requirements for commercial refrigerating appliances and ice-makers with an incorporated or remote refrigerant unit or, 2014.
[62] "BS EN ISO 9994:2019, Lighters - safety specification," no. March, 2019.
[63] "RT35 HC." https://www.rubitherm.eu/en/productcategory/organische-pcm-rt (accessed Jul. 18, 2025).
[64] G. Meramveliotakis, G. Kosmadakis, S. Karellas, Testing and characterisation of a scroll compressor with vapour injection using R454C as a drop in refrigerant in a water source heat pump, Int. J. Refrig. 176 (February) (2025) 359–372, https://doi.org/10.1016/j.ijrefrig.2025.05.006.
[65] R.V. Ravindran, D. Cotter, C. Wilson, M.J. Huang, N.J. Hewitt, An evaluation of the performance of a scroll machine in a reversible high-temperature heat pump - organic rankine cycle system using R1233zd(E) as the working fluid, Int. J. Refrig. 174 (December 2024) (2025) 321–332, https://doi.org/10.1016/j.ijrefrig.2025.03.013.
[66] H. Wang, et al., Numerical analysis of scroll compressor with combined profiles and intermediate discharge valve, Appl. Therm. Eng. 275 (March) (2025) 126928, https://doi.org/10.1016/j.applthermaleng.2025.126928.
[67] J. Chen, L. Tao, L. Huang, X. Wang, X. Li, H. Chen, Simulation and experimental study on the oil circulation rate (OCR) of R290 electrical vehicle compressors, Appl. Sci. 15 (3) (2025) 1–18, https://doi.org/10.3390/app15031391.
[68] S. Preisinger, et al., Experimental investigation of heat pump modules limited to 150 g of refrigerant R290 and a dedicated test rig, Energies 18 (10) (2025) 1–17, https://doi.org/10.3390/en18102455.